Modeling and Simulation of Dynamics of Polymeric Solutions: Progress and Challenges

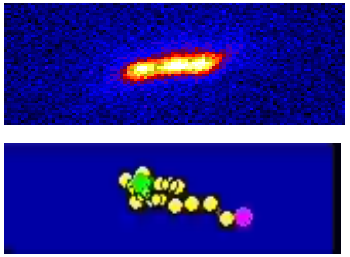

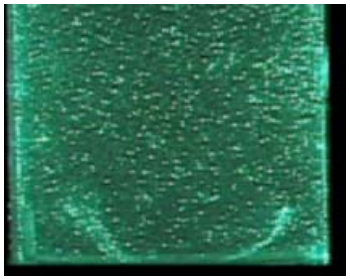

Bamin Khomami

Materials Research and Innovation Laboratory

Department of Chemical and Biomolecular Engineering,

University of Tennessee

Knoxville, TN, U.S.A

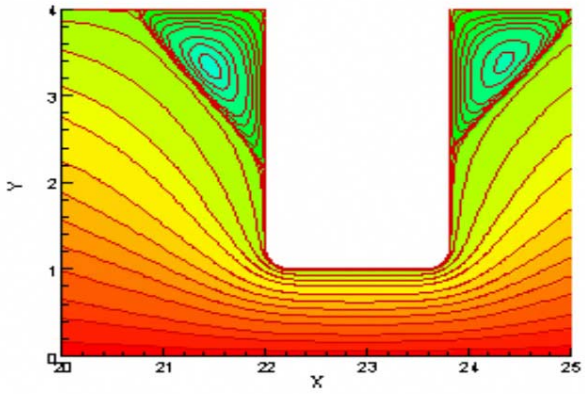

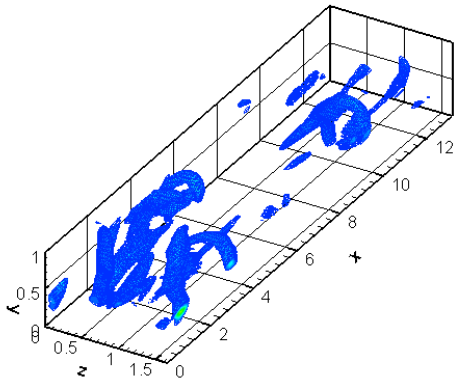

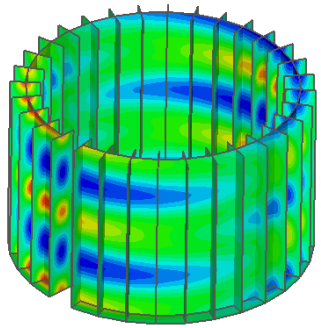

Outline

- General Introduction to Flow Behavior of Complex Fluids
- Modeling Dynamics of Dilute Polymeric Solutions
  - Introduction to kinetic theory based microstructural models
  - Flow induced chain Scission
  - Configuration based reduced order model
  - Summary and outlook
- Self Consistent Multiscale and Continuum Flow Simulation of Dilute Polymeric Fluids
  - Brief overview of computational techniques
  - Frictional drag properties of complex kinematics flows
  - Stability and flow transitions
  - Summary and outlook

Flow Properties of Newtonian and Complex Fluids

Newtonian Fluids: Homogenous 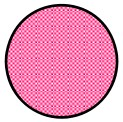

Complex Fluids: Microstructured 

Dimensionless Groups

Deborah Number, De: The ratio of the average fluid relaxation time to a flow time scale.

Wiessenberg Number, Wi: The ratio of elastic to viscous forces.

Direct visualization of microstructure evolution under flow: λ-DNA; Wi ~ 20.

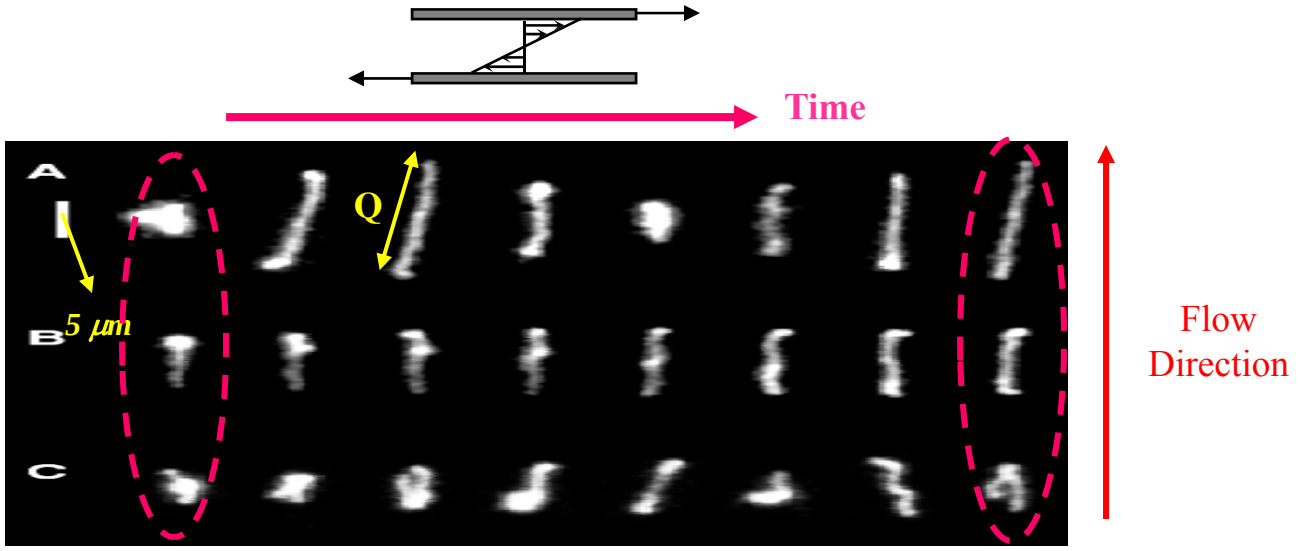

- **Flow is steady but due to Brownian fluctuations and entropic relaxation the instantaneous configurations are time-dependent. In addition, the unraveling speed is a strong function of initial configuration (*molecular individuality*).**
- **Microstructure evolution manifests itself as *viscoelastic* flow behavior. The macroscopic viscoelastic stress is a function of <*QQ*>.**

Flow Phenomena in Microstructured Fluids

Microstructure Development During Flow

Rheological Characterization

Taylor-Couette instability

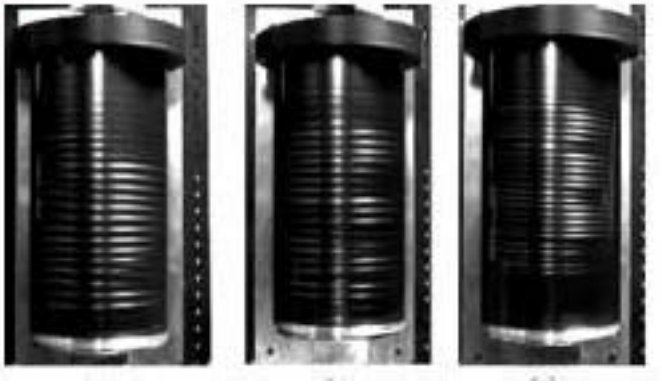

Muller, Larson, and Shaqfeh, 1989

Ribbing in coating flows

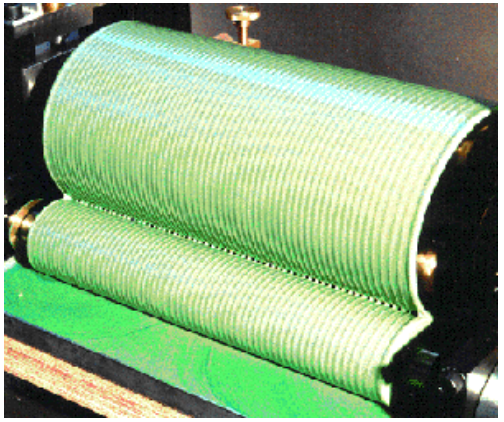

Lee, Grillet, Shaqfeh, and Khomami (1998)

Processing

Motivation and Goal

➢ Understanding dynamics of macromolecular solutions under external forcing such as hydrodynamic forces/electrical fields play an important role in many physico-chemical and biological systems. In addition, the ability to induce the desired microstructure in complex fluids through manipulation of the external field is to a great extent responsible for many useful products made of polymeric materials.

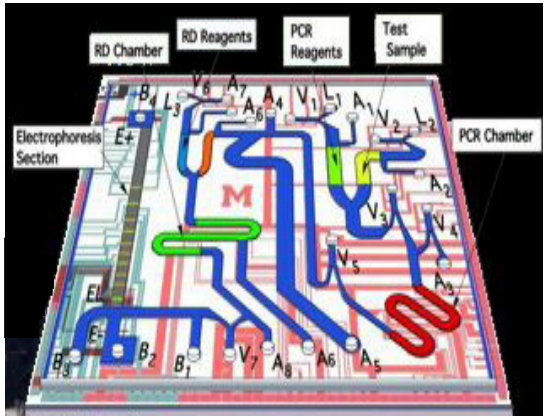

PCR/ Electrophoresis (Burns, Michigan)

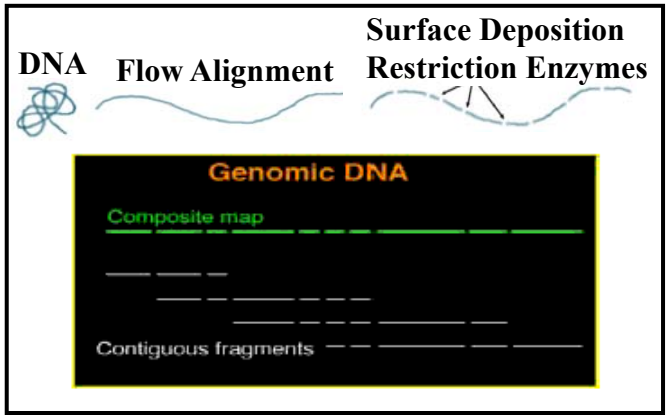

Optical Mapping (Schwartz, Wisconsin)

Our goal is to develop experimentally validated multi-scale models and simulations techniques to obtain quantitative understanding of dynamics of macromolecular solutions under external forcing (e.g., transport mechanics and flow transitions and nonlinear dynamics).

1. Modeling Dynamics of Dilute Polymeric Solutions
    1.1. Kinetic theory based microstructural models: A review
    1.2. Flow induced chain scission
    1.3. Configuration based reduced order model
    1.5. Summary and Outlook

Dilute Polymeric Solution

➢ Modeling and Simulation of Macromolecular Dynamics

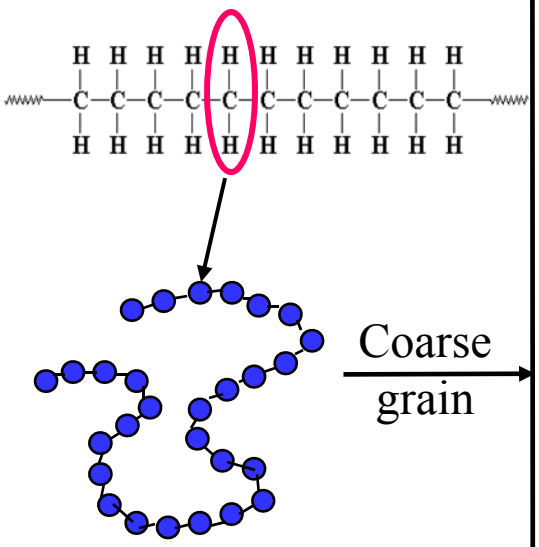

NEMD using united atom models limited to very short chains

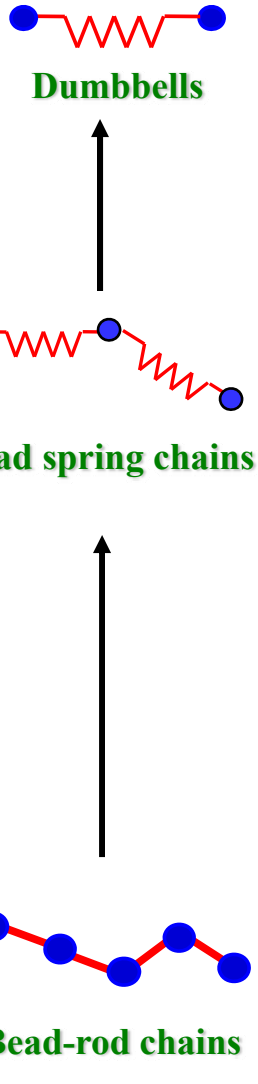

- FENE, Hookean, WLC, ILC, ALS
- Closure approximations – constitutive models e.g. Oldroyd-B, FENE-P, FENE-L, FENE-LS

- Flexible polymers – e.g. FENE, ILC, Hookean
- Semiflexible polymers – e.g. WLC

$$\frac{\vec{F}}{\left(kT/A\right)} = \left[\frac{C - D\left(Q/Q_o\right)^2}{1-\left(Q/Q_o\right)^2}\right]\frac{\vec{Q}}{Q_o}$$

C & $D = F(v)$

$$v = \frac{N_k - 1}{N_s}$$

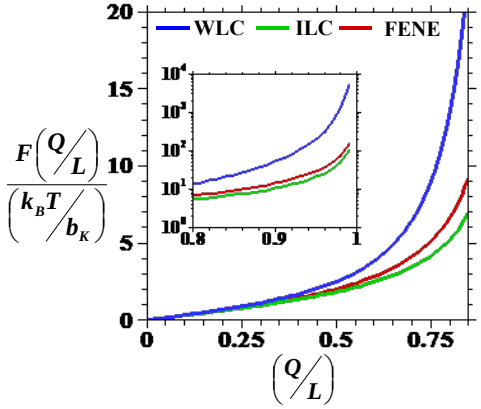

- Freely jointed/rotating chains – e.g. Kramers chain
- Semiflexible polymers – modeled as inextensible Wormlike chains with a bending potential; e.g. Porod-Kratky chain

Bead-Rod & Bead-Spring Descriptions

➢ DNA in high salt conc. >10mM & fluorescent dye YoYo-1; λ-phage, 21-22 μm, l_p= 66-70, K=150-160.

"Molecular Individualism"
Configurations observed in steady shear

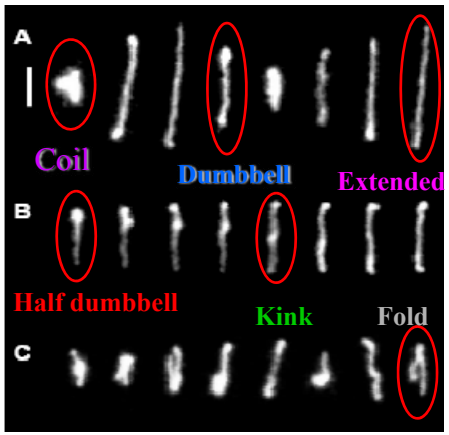

Tumbling dynamics in shear

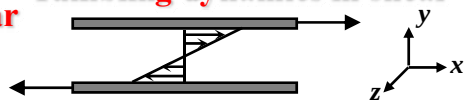

Velocity-gradient Plane (*x*-*y*)

$f_{tumb} \sim Wi^{0.62}$

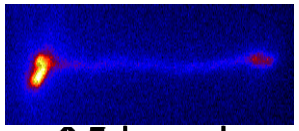

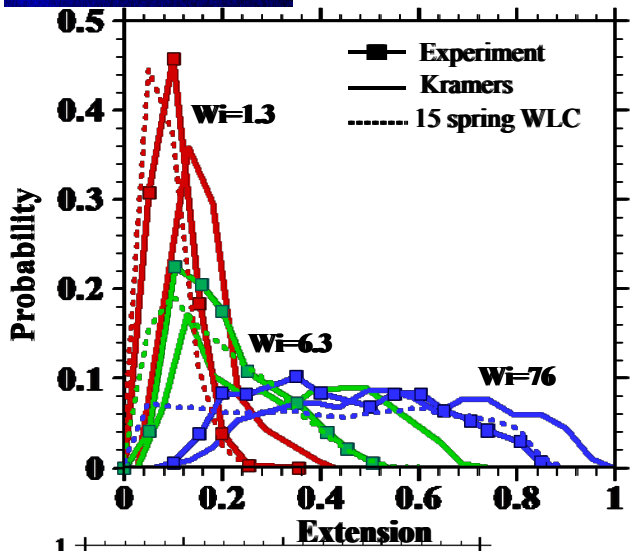

Experiments Simulation

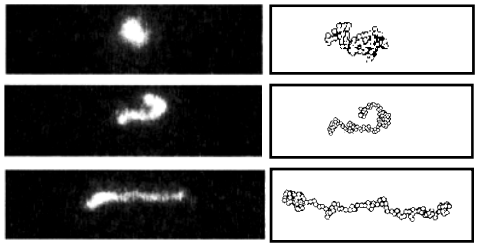

Single molecule video fluorescence microscopy and Brownian dynamics simulations (cross-slot flow)

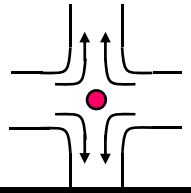

Planar extensional flow

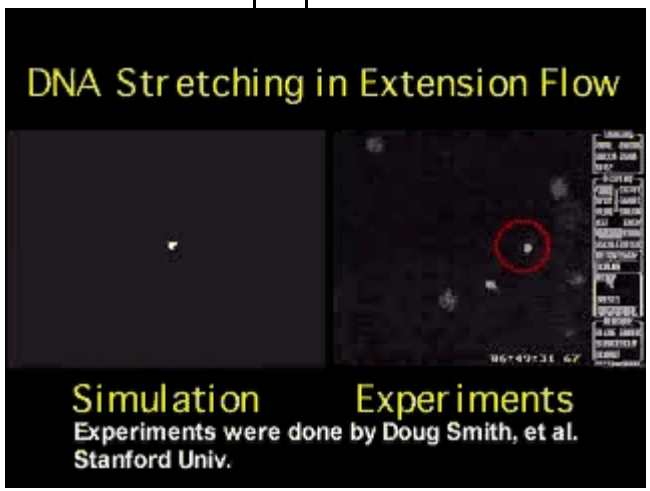

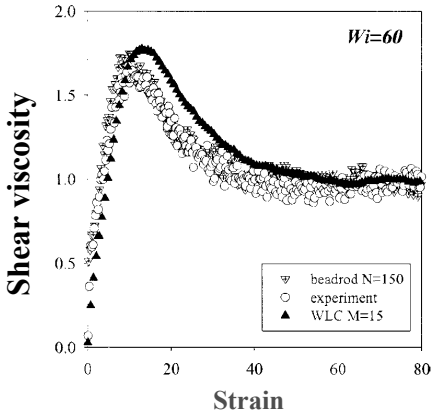

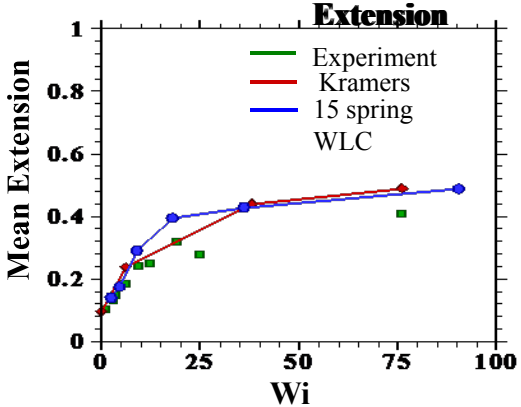

Expansion factor in uniaxial extensional flow

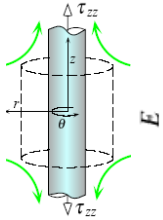

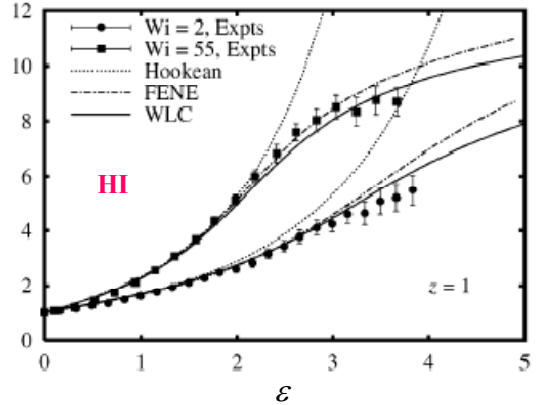

Dumbbell Description

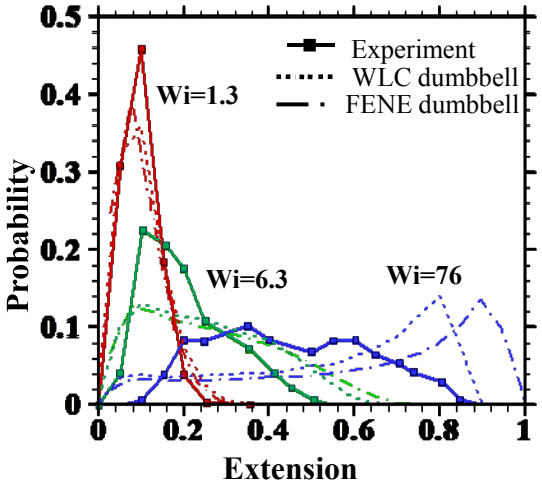

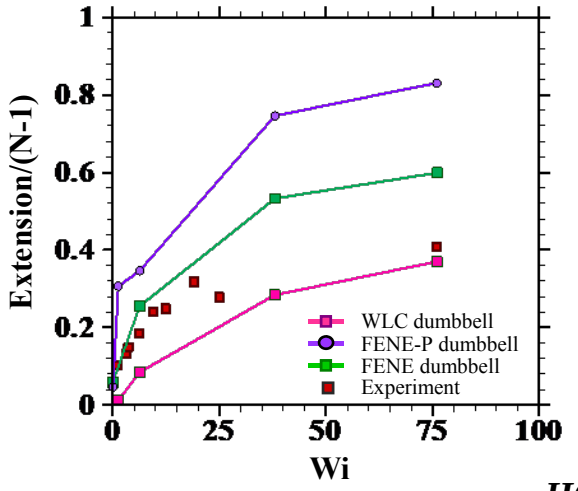

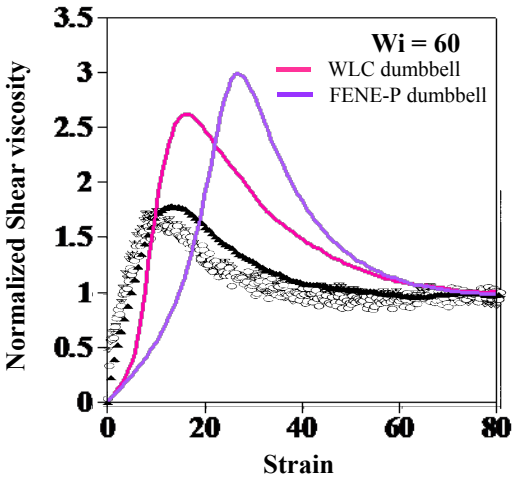

Closed Form Constitutive equation: FENE dumbbell force law

$$\vec{F} = \frac{H\vec{Q}}{1 - \frac{Q^2}{b}} \xrightarrow{\text{Replace}} \langle QQ \rangle$$

$$\frac{d\langle QQ \rangle}{dt} - \kappa \cdot \langle QQ \rangle - \langle QQ \rangle \cdot \kappa^T = \delta - \frac{\langle QQ \rangle}{1 - \langle QQ \rangle / b}$$

FENE-P constitutive equation

- Elastic dumbbell models and closed from constitutive equations can at best provide qualitative predictions of the macromolecular dynamics even in homogenous kinematics flows.
- Bead-rod and bead-spring models with sufficient internal degrees of freedom can predict both the dynamics of individual polymer molecules as well as the macroscopic rheological properties of dilute solutions with good accuracy in simple kinematics flows.

Flow Induced Macromolecular Scission

- Motivation: To understand the influence of flow type and strain rate on macromolecular scission. (Narrow MW polymers; Turbulent drag reduction by polymers; Sequencing and lab on a chip devices, etc..).
- Experimental findings: In steady extensional flow the critical strain rate $\propto MW^{-2}$ (Odell & Keller, 1986).

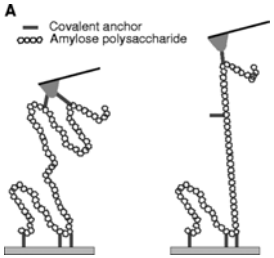

Bond Rupture Studies
AFM Studies: (Grandbois et al., Science, 1998)

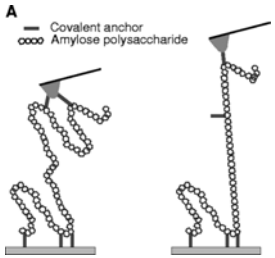

- Force vs. extension has complex behavior over length scales of O(1) nm
- Bond scission is a stochastic process, i.e., fluctuations play an important role in determining bond scission

Number of rupture events vs. force

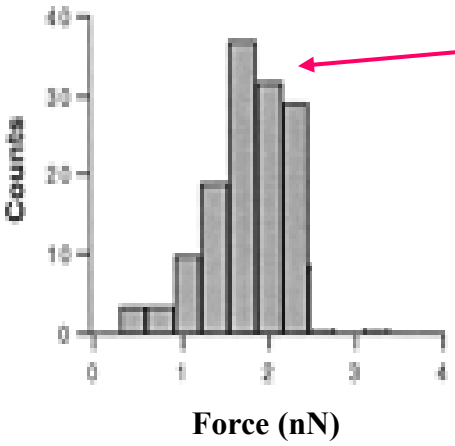

Force vs. chain extension

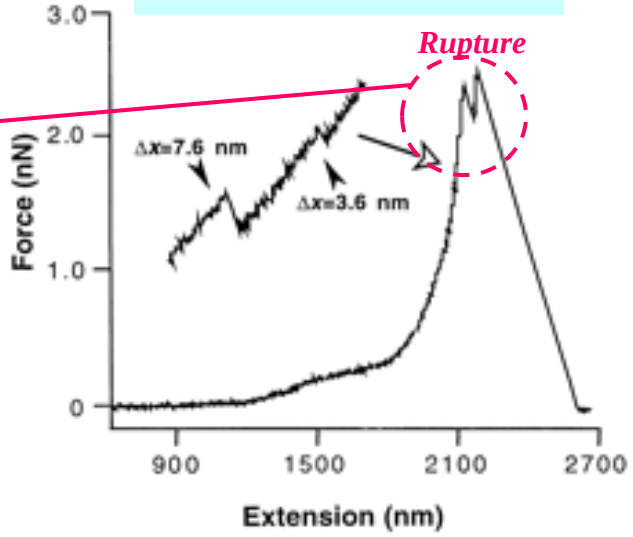

Flow Induced Macromolecular Scission

➢ Objective: Develop an hi-fidelity simulation algorithm for the prediction of flow-induced chain scission. Specifically, we will use the bead-rod description and incorporate the effect of force/tension fluctuations on scission.

➢Stochastic Scission Algorithm: Detailed study of statistical properties of tension using BD.

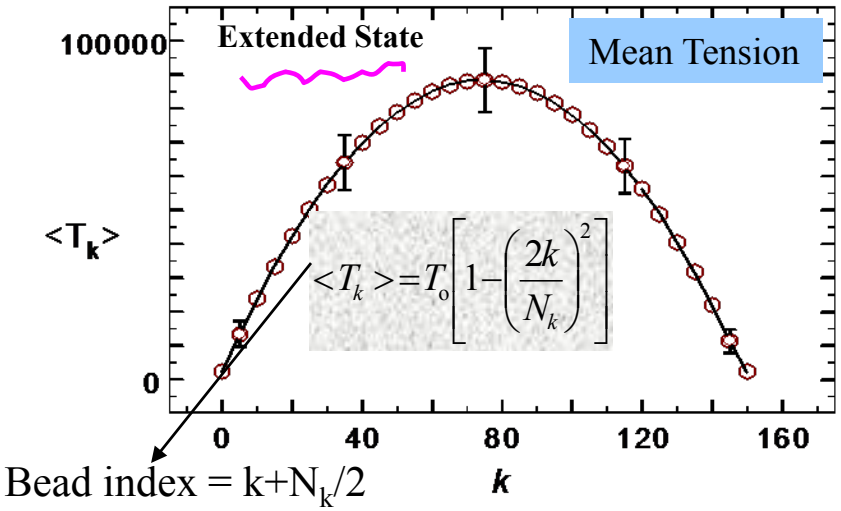

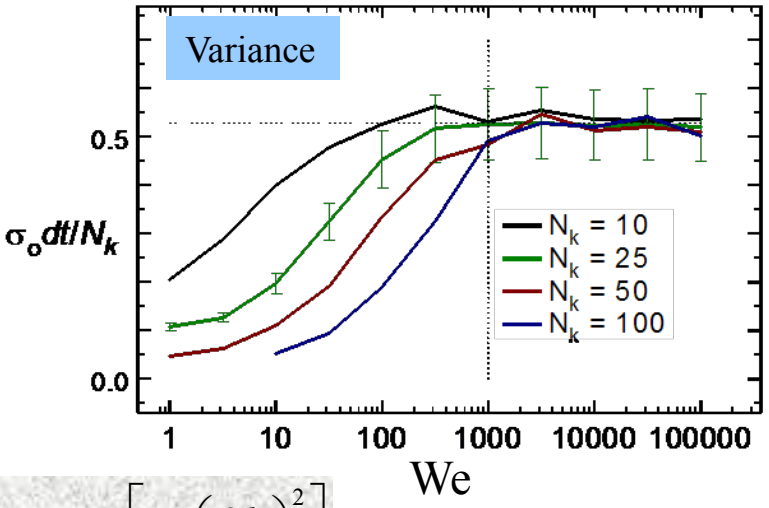

$$T_o = 0.125\,\dot{\varepsilon}\,N_k^{\,2}(\zeta\,a^2/k_BT) = 8.82\cdot We$$

$$\sigma_k^2 = \sigma_o\cdot\left[1-\left(\frac{2k}{N_k}\right)^2\right]$$

$$\sigma_o = N_k/(2dt)$$

$$\text{Mean:}\langle T_k\rangle = 8.82\,We\left[1-\left(\frac{2k}{N_k}\right)^2\right] \quad \text{Variance:}\sigma_k^2 = \frac{N_k}{2\,dt}\left[1-\left(\frac{2k}{N_k}\right)^2\right],\ We>1000$$

Flow Induced Macromolecular Scission

➢ **Probability of scission is evaluated using a Gaussian p.d.f. (Grandbois et al. 1999).**

Example: Critical tension value based on a C-C bond (≈ 4 nN) and $a \approx 100$ nm (stained DNA, Larson et al. 1999), $T_c/(kT/a) \approx 10^5$. ⇒ In steady elongational flow, $We_c \approx 12{,}000$.

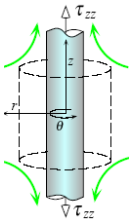

Chain Scission in Uniaxial Extensional Flow

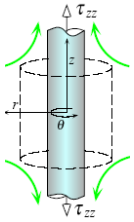

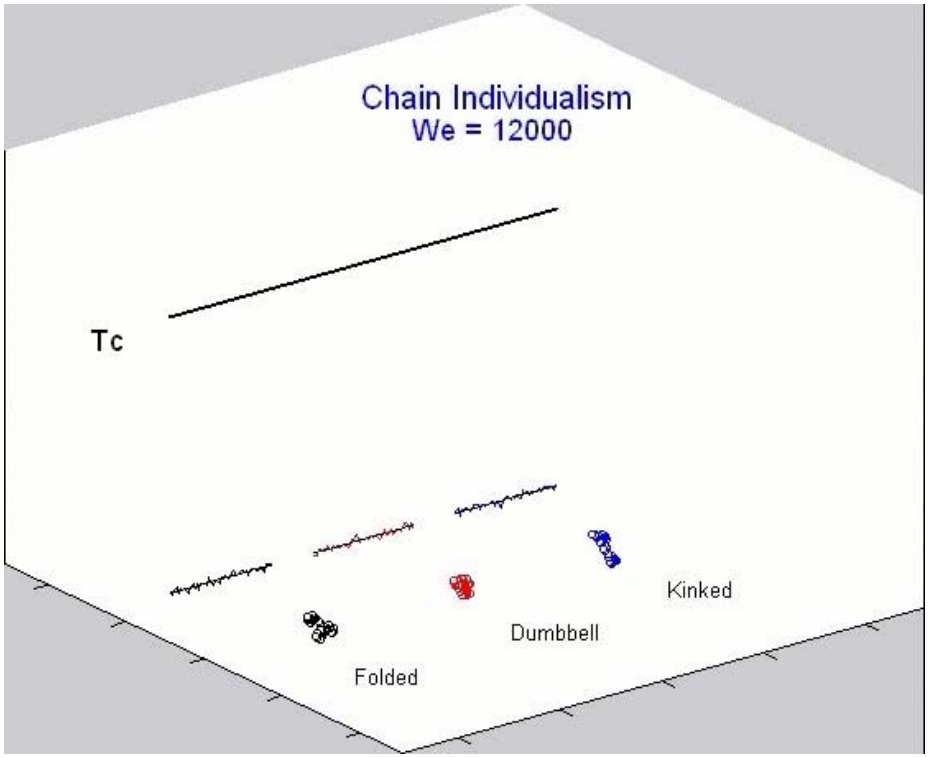

Midpoint Scission

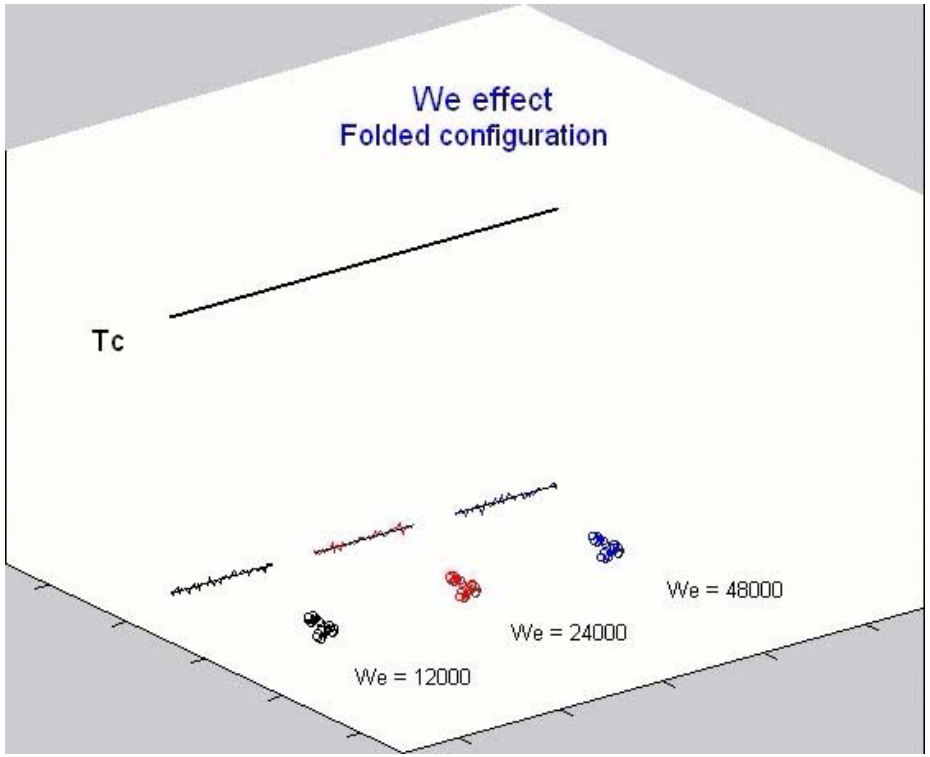

Complex Scission

Flow Induced Macromolecular Scission

➢ **Scission kinetics in uniaxial extensional flow**

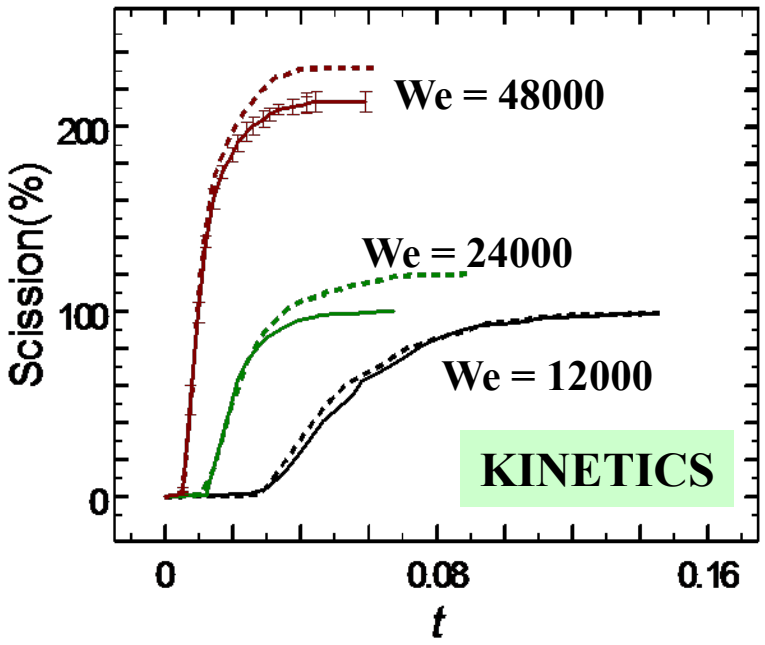

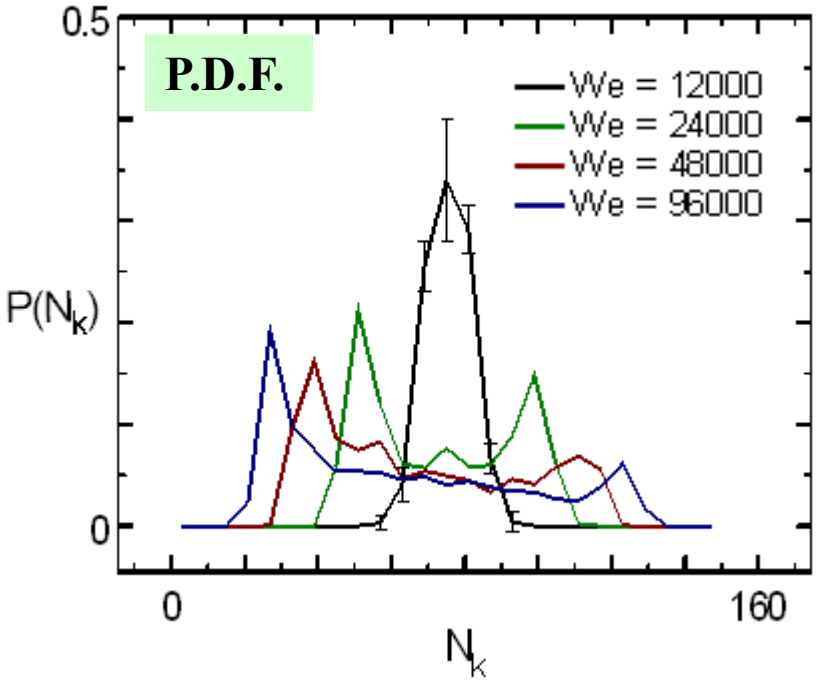

➢ Kramers chain predictions agree with the experimental observation: The critical strain rate ∝ MW^{-2} in steady extensional flows.

➢ Midpoint scission is only valid near the critical strain rate. For strain rates larger than the critical value, scission occurs closer to the chain ends. This happens because partially coiled configurations can break.

➢ Chain scission also occurs in transient shear flows. The critical strain rate is an order magnitude larger than uniaxial extensional flow. The critical strain rate ∝ $MW^{-1.5}$.

H. Sim, B. Khomami, R. Sureshkumar, JOR, 2007.

Flow Induced Macromolecular Scission

➢ **Scission kinetics in complex kinematics flows**

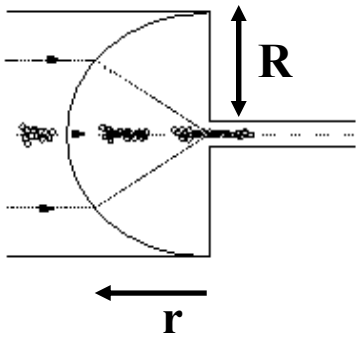

$$\dot{\varepsilon} = |\, 4Q / \pi\, r^3 \,|$$

$$-\infty < r / R \le 0.02$$

More scission events occur as the residence time increases. For residence times greater than 5% of the longest relaxation time:

$$\dot{\varepsilon}_c \propto N_k^{-1.75}$$

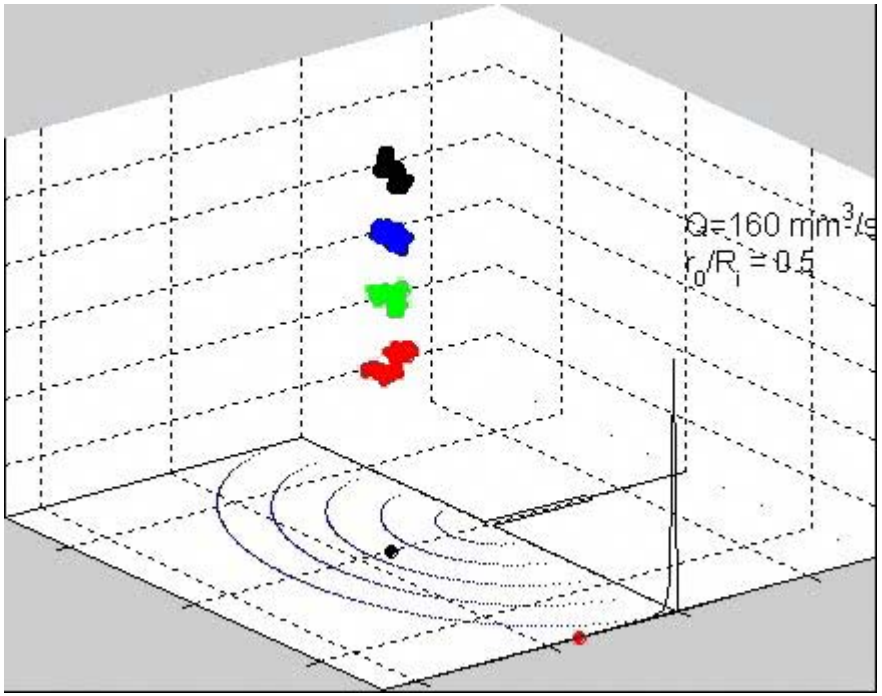

Current Research

Development of multiscale simulation strategies for chain scission under external forcing, i.e., determination of scission force via combined quantum and atomistic simulations.

A New Configuration Based Approach

Coarse-graining based on Configurations

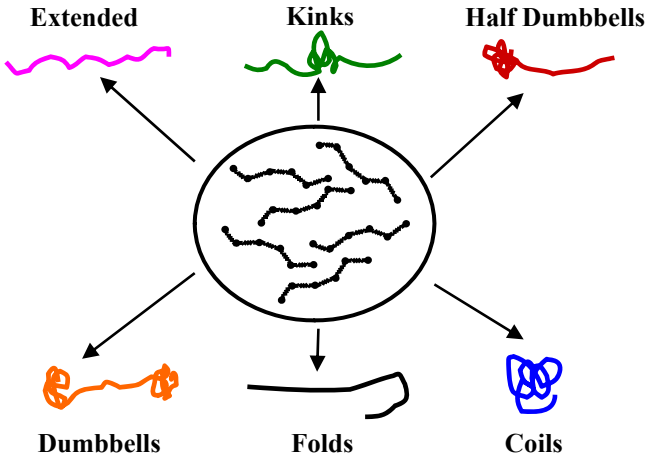

Configuration distribution in steady shear and uniaxial extensional flow

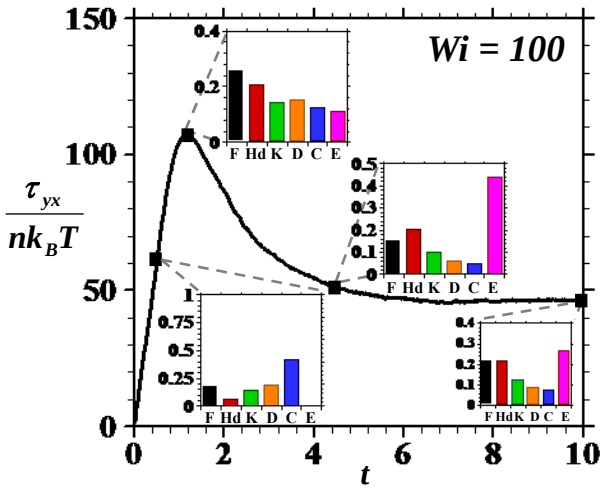

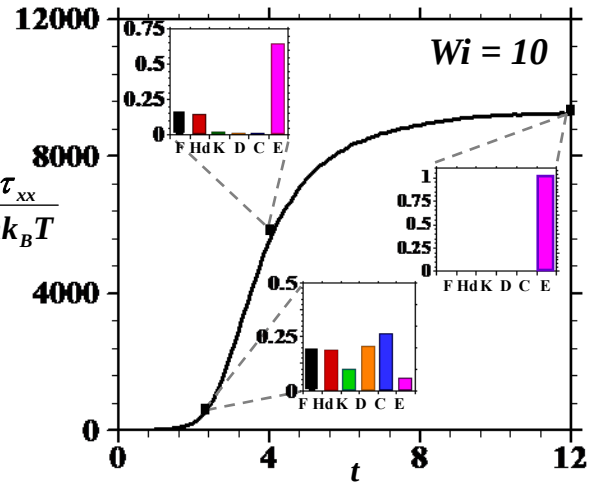

MAPPING CONFIGURATION SPACE

- The configuration landscape is partitioned into a few O(1) configuration classes
- An automated configuration sorting algorithm is used to classify configurations
- Various flow types and strengths are extensively sampled in order to generate the map for the configuration landscape in terms of the end-to-end vector

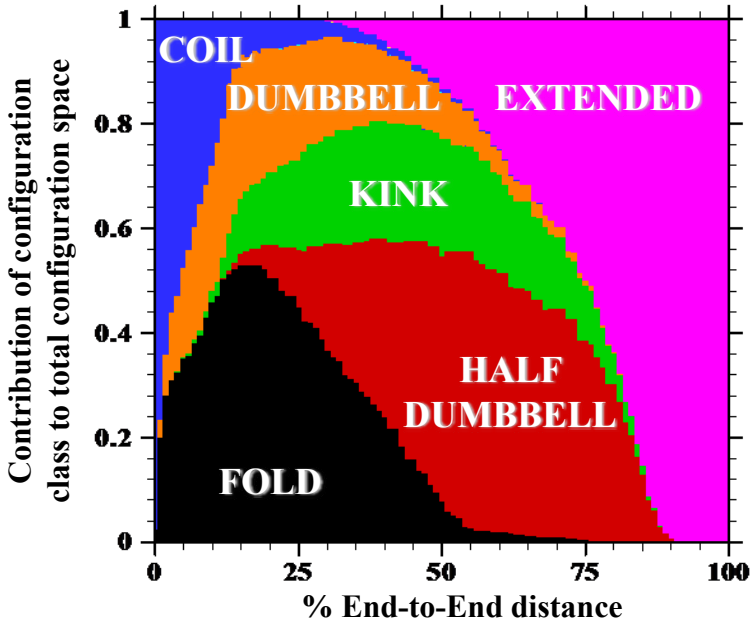

Unique Representation for Configuration Classes

- Configuration classes are modeled as dumbbells with a FENE force law
- Configurations are classified based on their drag coefficient, ζ

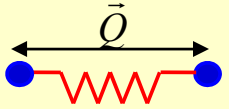

Coil: $u^{\infty} = U_1\,\hat{e}_x + U_2\,\hat{e}_y$; 2a ; $F_D = 6\pi\mu a[U_1\,\hat{e}_x + U_2\,\hat{e}_y]$; **Isotropic**

Stretched: $u^{\infty} = U_1\,\hat{e}_x + U_2\,\hat{e}_y$; 2a, 2b ; $F_D = 6\pi\mu a[C_{F1}U_1\,\hat{e}_x + C_{F2}U_2\,\hat{e}_y]$

Anisotropic: $\frac{C_{F1}}{C_{F2}} \to \frac{1}{2}$ as $\frac{b}{a} \to 0$

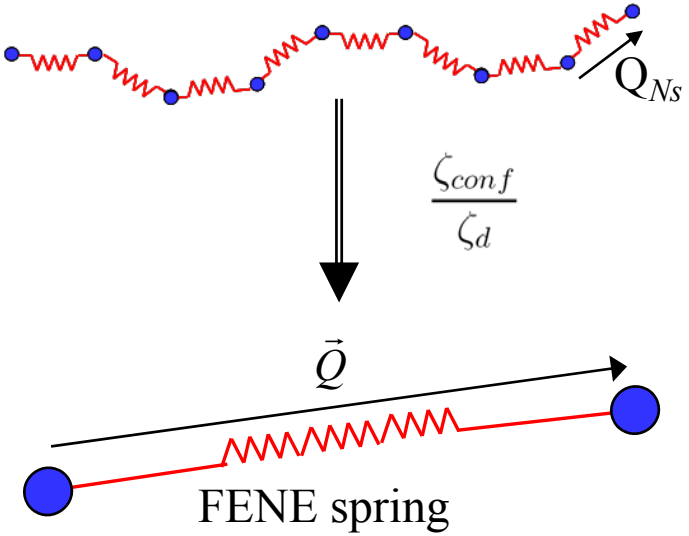

$$d\vec{Q} = \left[\kappa \cdot \vec{Q} - \frac{2}{\zeta}\vec{F}^{S}\right]\Delta t + \sqrt{\frac{2kT}{\zeta}}\,d\vec{W}$$

Write a force balance at each level of description to develop expression for the configuration specific drag.

Configuration Class	$\frac{\zeta_{conf}}{\zeta_d}$
Fold	3
Half Dumbbell	2
Kink	1.15
Dumbbell	4.3
Coil	1.15
Stretched	1.85

Configuration Based Model

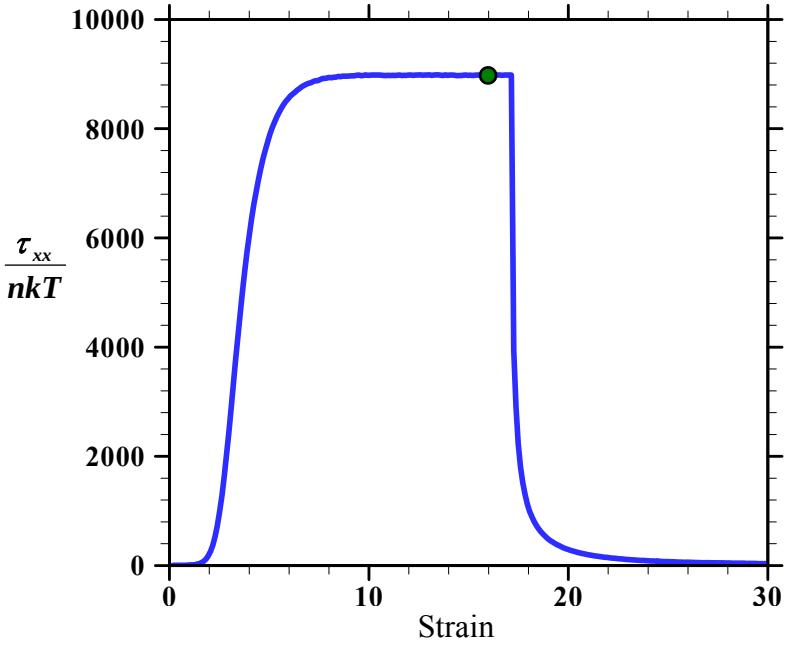


Folds


Half dumbbells


Kinks


Dumbbells


Coils

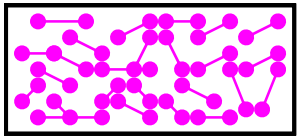
Extended

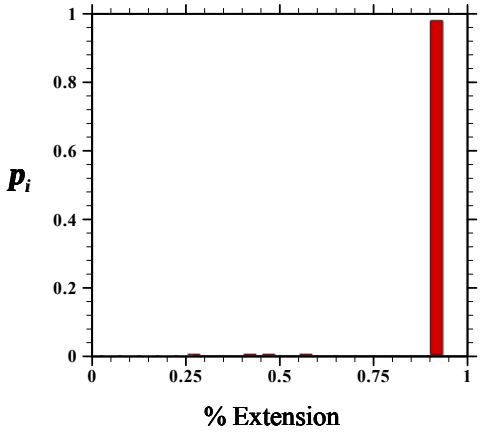

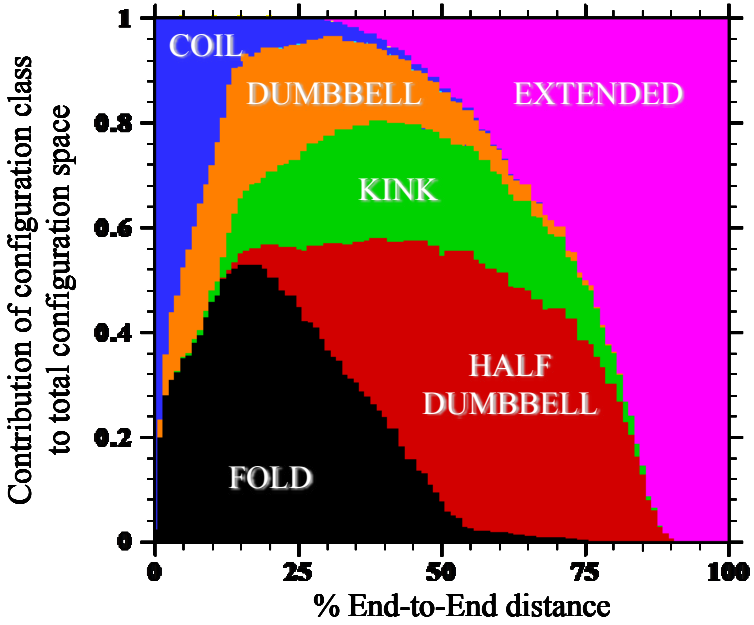

Configuration Based Model

STEADY SHEAR FLOW

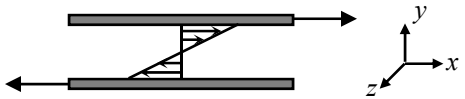

Velocity-gradient Plane (x-y)

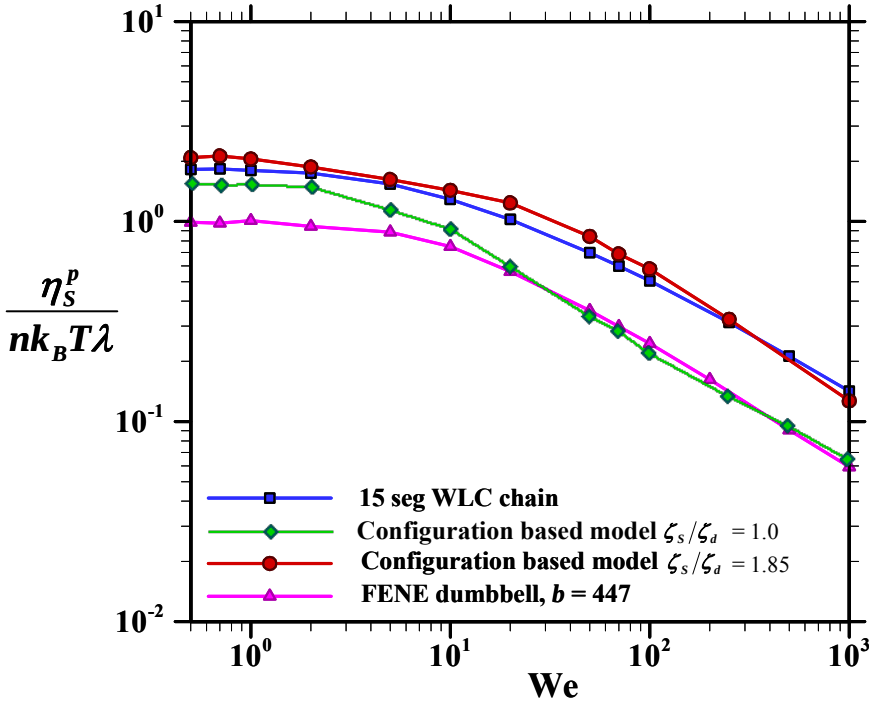

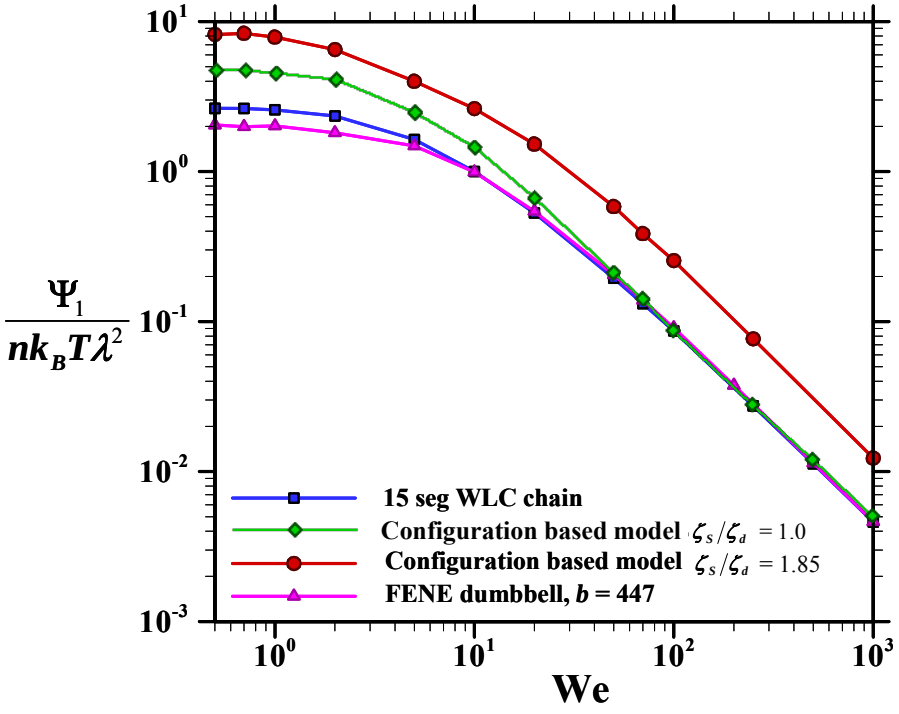

- **Shear viscosity for the configuration based model are in good agreement with the underlying bead-spring chain**
- **Normal stresses are overpredicted for all *We***
- **Zero-shear viscosity for the model with the modified drag coefficient for the stretched state is in agreement with the multi-bead-spring chain but underpredicts the viscosity at high *We***
- **Plateau first normal stress coefficient is overpredicted, but the high *We* first normal stress coefficient is in agreement with the multi-bead-spring chain**

Configuration Based Model

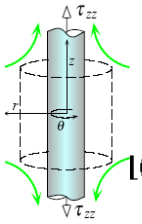

UNIAXIAL EXTENSIONAL FLOW

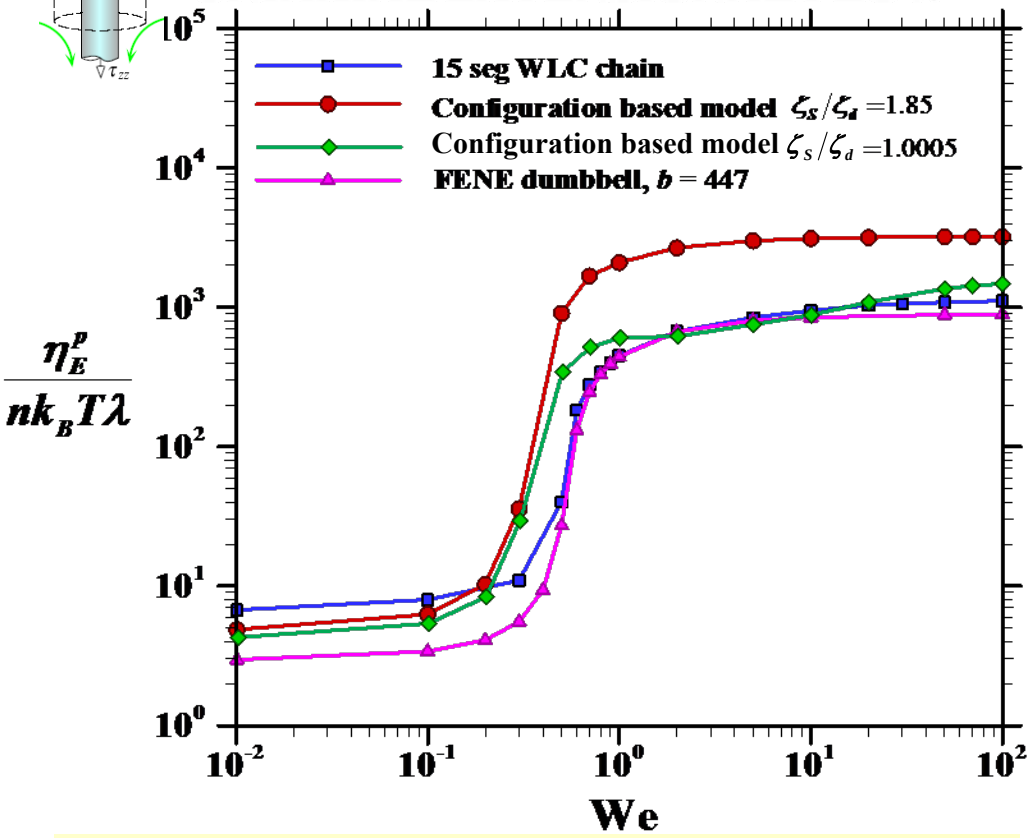

- Low *We* extensional viscosity is in good agreement with the multi-bead-spring chain but the coil-to-stretch transition and the high *We* plateau are over predicted.
- Modifying the stretched state drag coefficient leads to improved predictions for the high *We* plateau.

Model Improvements

$\eta \rightarrow \delta_y$

$\tau_{xx} \rightarrow (\vec{Q}\vec{Q})_{xx}$

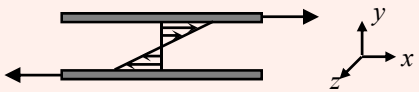

Velocity-gradient Plane (x-y)

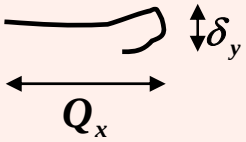

✓ δ_y is accurately predicted ⇨ configuration dependent drag coefficients are critical to accurate predictions for δ_y

✓ Q_x is over predicted ⇨ configuration dependent drag coefficients lead to over prediction of the extension in the flow direction

⇩

Anisotropic drag coefficients

V. Venkataramani, R. Sureshkumar and B. Khomami, JOR, 2008.

Summary and Outlook

Although tremendous progress in modeling and simulation of dynamics of polymeric solutions has been made, number of issues deserve further consideration,

- Quantitative modeling of long range hydrodynamic interactions for long chains and detailed comparison with experiments both in bulk and interfacial flows.

- Single molecule experimental studies utilizing fluorescently labeled synthetic polymers and complimentary BD simulations to examine polymer dynamics over a broad range of molecular architectures and flexibility.

- Accurate coarse grained and reduced order models for polymer dynamics.

2. Self Consistent Multiscale and Continuum Flow Simulation of Dilute Polymeric Fluids

- 2.1. Brief overview of computational techniques
- 2.2. Frictional drag properties of complex kinematics flows
- 2.3. Stability and flow transitions
- 2.4. Summary and outlook

Multiscale Simulation Strategy

Continuum Level Governing Equations
(FEM, Spectral)
- Hydrodynamics
- Electric/Magnetic Field

Mesoscopic Level Description of Microstructure
(BD, FP)

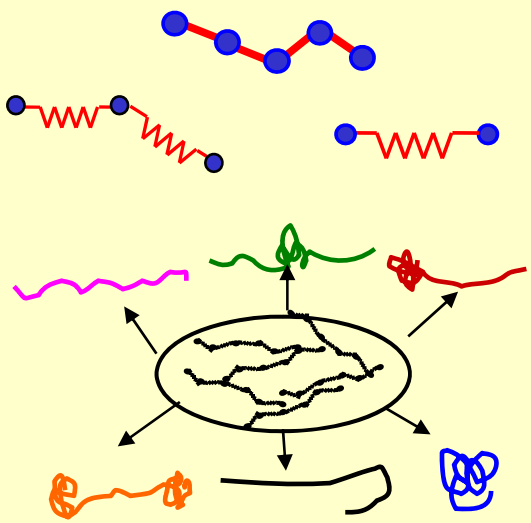

Self Consistent Dynamic Simulator

Constitutive Equation
$\tau = f(\dot{\gamma}); q = f(\Delta T)$

Closure Approximation

$$\tau + \lambda\left(\frac{\partial \tau}{\partial t} + \boldsymbol{u}\cdot\nabla\tau - \nabla\boldsymbol{u}^T\cdot\tau - \tau\cdot\nabla\boldsymbol{u}\right) = 2\eta_P\dot{\gamma}$$

Continuum ⟷ ***Multi-Scale***

Atomistic Level Description
(NEMD)

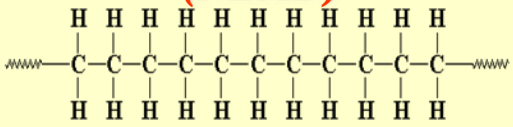

Simulation Fidelity to a Great Extent Depends on Fidelity of the Microstructural Evolution Model

Complex Kinematics Flows of Dilute Polymeric Solutions

Despite significant progress in the past two decades, complex kinematics flow computations of dilute polymeric solutions with closed form constitutive equations or simple micromechanical models, such as the elastic dumbbell model, are still incapable of providing quantitative description of essential flow dynamics, such as frictional drag, and vortex structure. A few examples include long standing benchmark mark flow problems, namely sedimentation of a sphere in a tube and contraction/expansion flows.

4:1:4 Axisymmetric Contraction-Expansion Flow of Dilute Polymeric Solutions

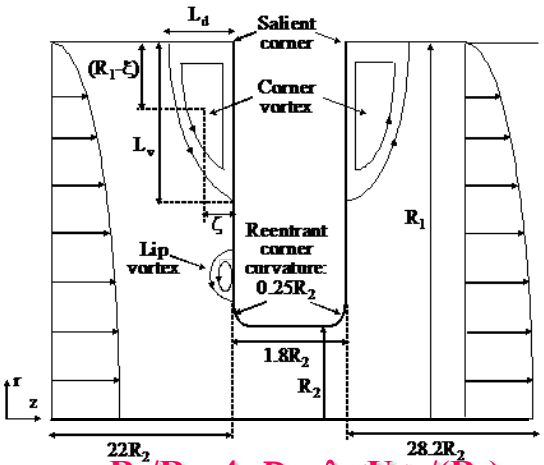

$R_1/R_2=4$; $De=\lambda<U_2>/(R_2)$

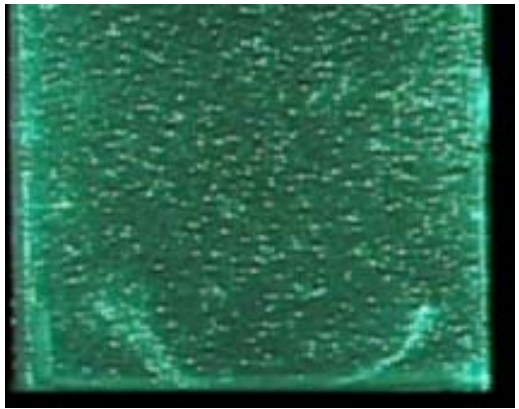

Flow Direction

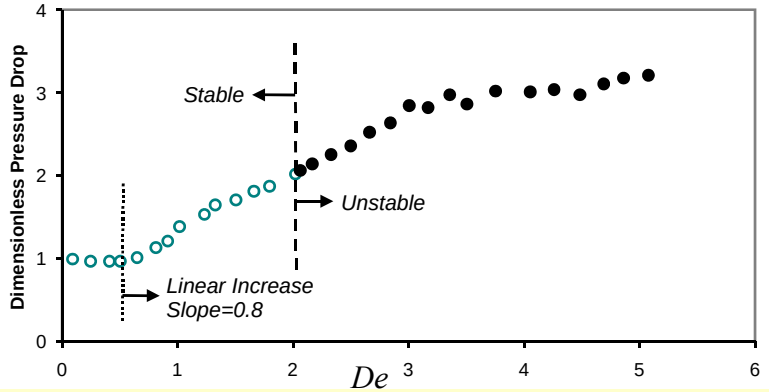

- Numerical simulations have generally predicted a reduction in the pressure drop as *De* is enhanced. A 10% increase in the pressure drop has been observed with unrealistically low finite extensibility parameters.
- Experimental studies have demonstrated different vortex evolution pathways as a function of the polymer extensibility.

Quantitative prediction of friction drag properties of dilute polymeric solutions in complex kinematics flows remains a challenge.

Multiscale Simulation: 4-1-4 Contraction& Expansion

The success of bead-spring chains in describing individual chain dynamic and rheology of dilute polymeric solutions has motivated us to perform multiscale self-consistent flow simulations with bead-spring chains. Of particular interest is the elucidation of the mechanism leading to the experimentally observed pressure enhancement. The influence of macromolecular chain extensibility on the vortex dynamics will also be briefly discussed.

➢ Rheology: 0.025 wt% PS/PS (Rothstein & McKinley (1999))

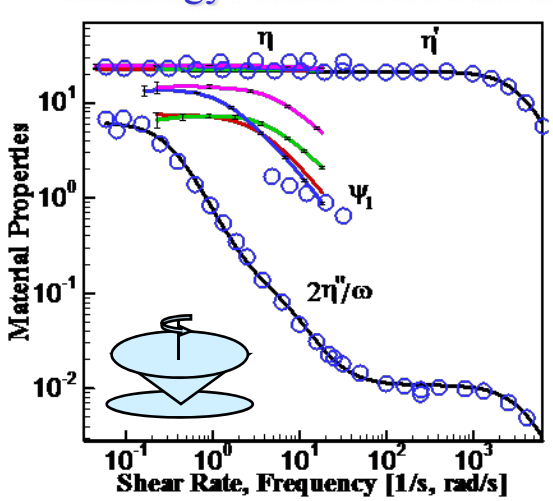

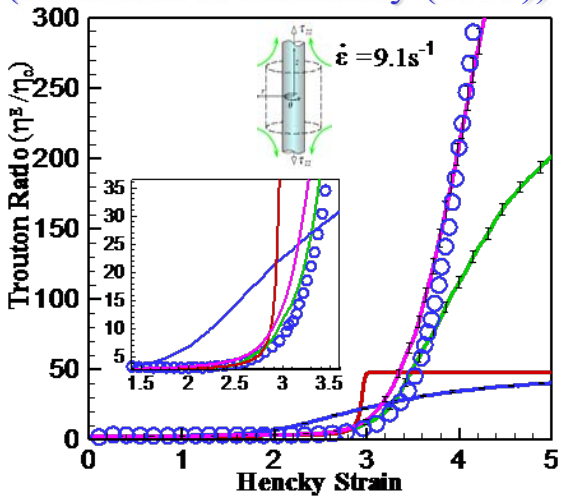

FENEP b=300
3seg FENE b=225
1seg FENE b=1800
3seg FENE b = 4500
Experimental Data

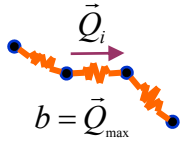

Strain Range ~ 2.5-4

Mode (i)	η_i (Pa.s)	λ_i (s)
1	1.0695	2.8742
2	0.3509	0.1312

$$\lambda_m = \sum_{i=1}^{2} \eta_i \lambda_i \Big/ \sum_{i=1}^{2} \eta_i = 2.197 \text{ s}$$

➢ Computational Details

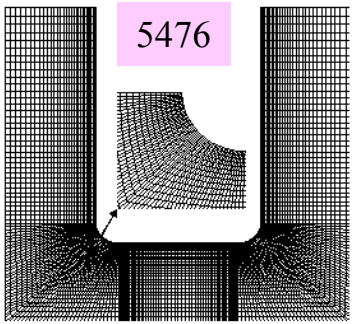

Variable(s)	DOF: 2736 Elements	DOF: 5476 Elements
$\vec{u}$	11,279	22,373
P	2,904	5,711
$\underline{\underline{G}}$, and $\underline{\underline{\tau}}$	11,616	22,844
$\vec{Q}: N = 1, N_f = 1024$	8,921,088	17,544,192
$\vec{Q}: N = 3, N_f = 960$	25,090,560	49,343,040

Pressure Drop and Vortex Dynamics

Experiments (Rothstein & McKinley, 1999)

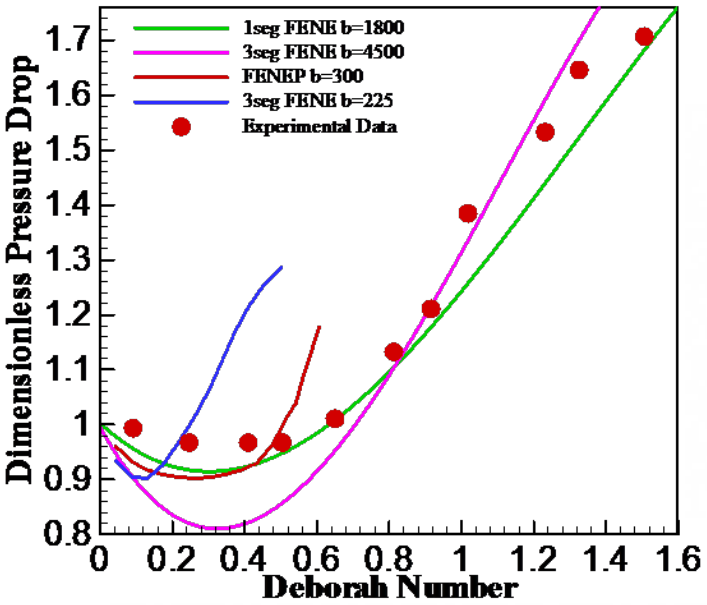

3Seg FENE b=225 vs. De

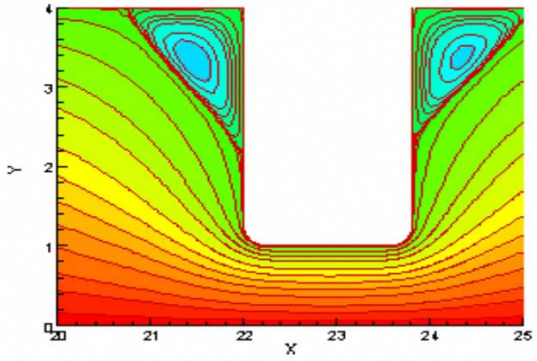

FENEP b=300 vs. De

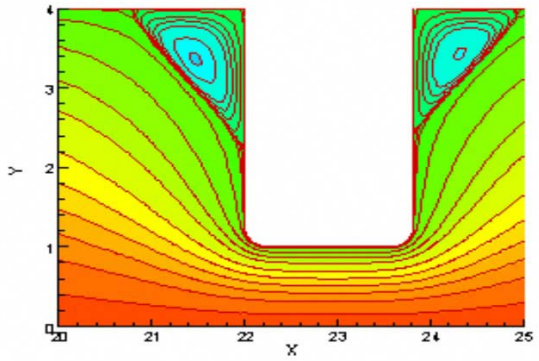

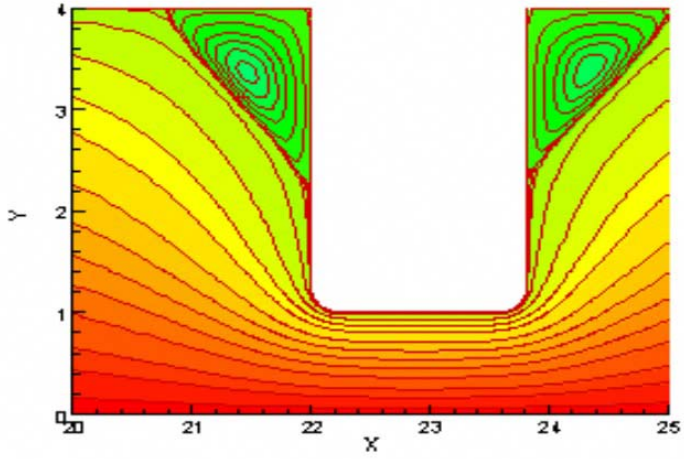

1Seg FENE b=1800 vs. De

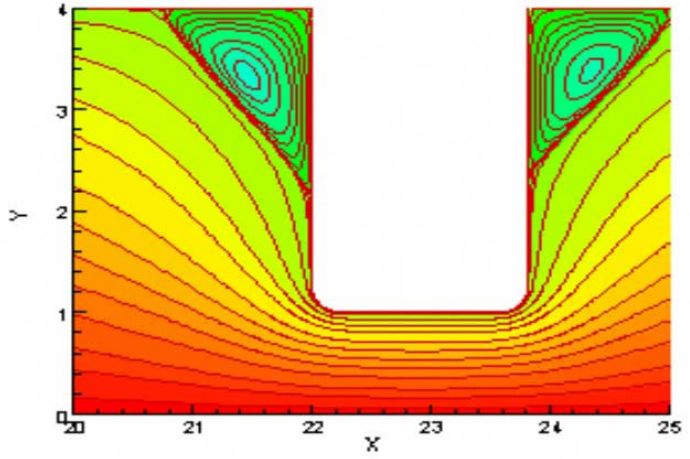

3Seg FENE b=4500 vs. De

Rate of Stress Work

➢Rate of stress work: $\dot{W} = \int_V \underline{\underline{\pi}} : \vec{\nabla}\vec{u}\, dV$; $\vec{u}$: fluid velocity of the fluid, $\underline{\underline{\pi}}$: total stress tensor

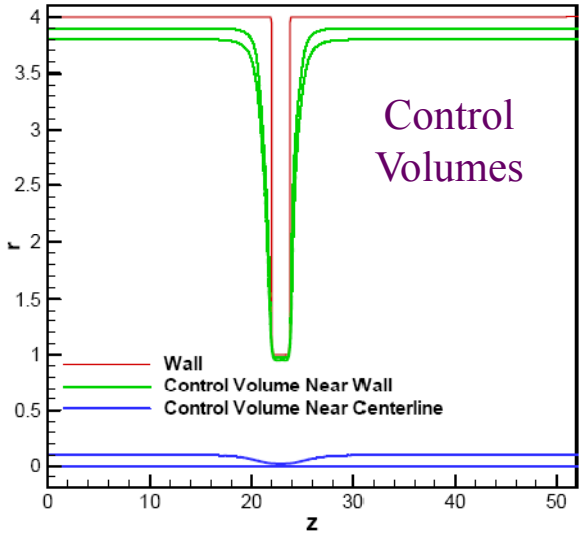

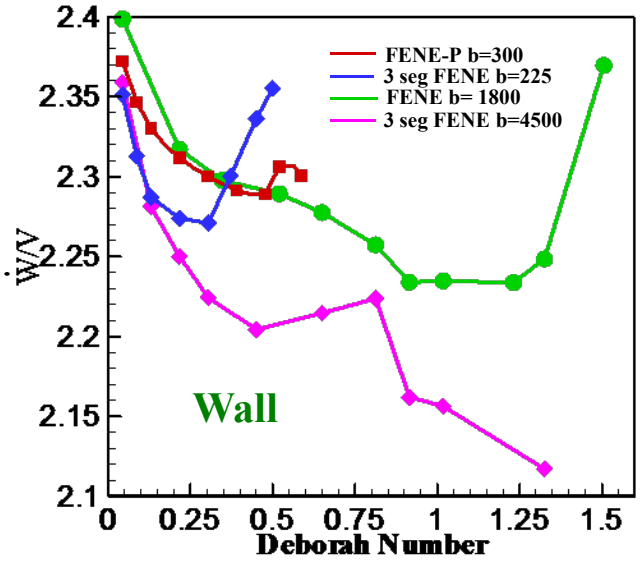

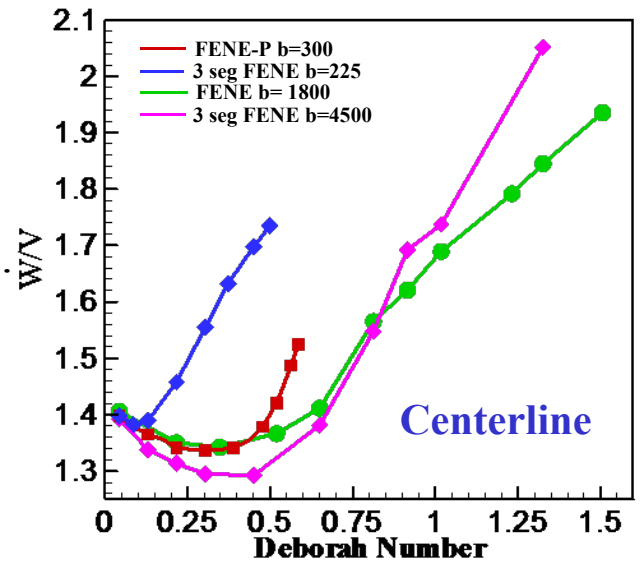

The flow near the centerline is controlling the pressure drop enhancement. Significant implications in design of extensional rheometers for dilute polymeric solutions.

Rate of Stress Work: Elastic & Viscous

Total Stress (π)= Elastic Stress (Σ)+Viscous Stress (τ_{pv})+ Solvent Stress (τ_s)

Elastic Stress Work: $\int_V \Sigma : \nabla u \, dV$

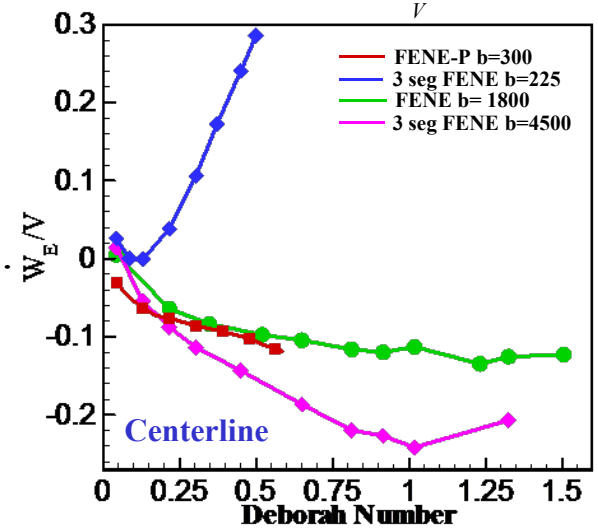

Viscous Stress Work: $\int_V \left(\tau_{pv} + \tau_s\right) : \nabla u \, dV$

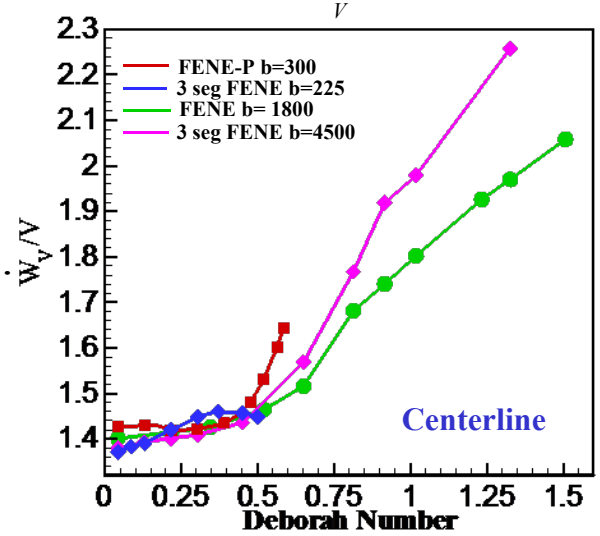

- Pressure drop enhancement (PDE) for the low *b* FENE models is occurring due to elastic stress energy dissipation.
- PDE for the high *b* FENE models and the FENE-P model is occurring due to the polymer induced flow modification.
- Negative values for the rate of elastic stress work for the high *b* FENE models and the FENE-P models demonstrate that the flow kinematics/microstructure coupling results in energy recovery.

A. Koppol, R. Sureshkumar and B. Khomami, JNNFM, 2007.

A. Koppol, R. Sureshkumar and B. Khomami, JFM, In Press 2008.

Summary and Outlook

- Multiscale simulations with micromechanical models with sufficient internal degrees of freedom are capable of providing an accurate description of complex kinematics flow of dilute polymeric solutions.
- Despite significant algorithmic advances to date, this class of multiscale simulations still remains extremely CPU intensive. Hence, wide spread use of this class of simulations in both academic and industrial settings requires further research in developing hi-fidelity coarse grained model and of further algorithmic advances.

Overview of Elastically Driven Flow Instabilities

➢ Observations:

Viscoelastic nature of polymeric liquids can significantly affect onset conditions and post critical dynamics of flows that are unstable due to inertial or capillary forces. In addition, it has been shown that viscoelastic forces can give rise to new mechanisms of instability, "purely elastic instabilities":

➢ Unidirectional Flows:

Curvilinear Flows (e.g., Taylor-Couette/Dean, Plate/Cone and Plate): Coupling of streamline curvature and normal stresses gives rise to purely elastic instabilities.

PIB Boger Fluid; Parallel Plate Geometry
McKinley, Armstrong& Brown (1991)

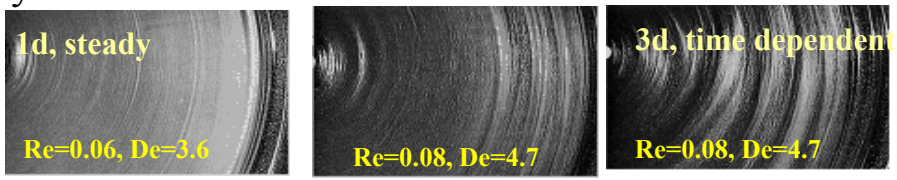

In addition, for thermally sensitive polymeric solutions (viscosity and relaxation time is a strong function of temperature), coupling of perturbation radial velocity and the base state temperature gradient (arising either from viscous dissipation or externally imposed temperature gradient) that gives rise to reduced dissipation and hence destabilization, "thermo-elastic instabilities"

Al-Mubaiyedh, Thomas, Sureshkumar, Khomami (1999-2005)

Interfacial and Free Surface Flows (e.g., Multilayer pressure and drag driven rectilinear flows): Jump in the normal stresses across interfaces and/or the free surface).

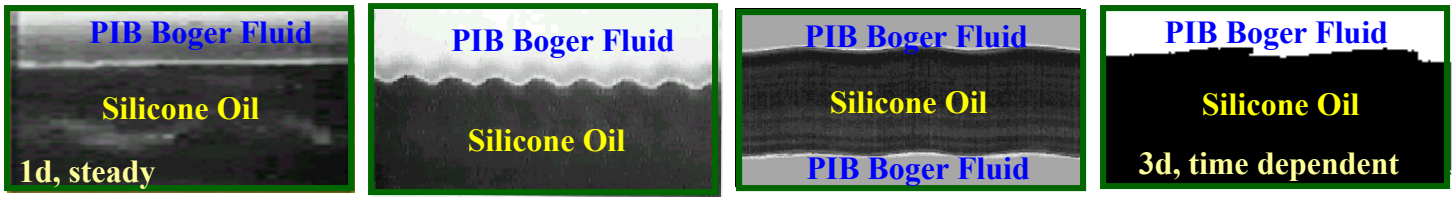

Pressure driven channel flow: Su and Khomami (2000)

Our understanding of elasticity driven unidirectional flow instabilities has reached a mature level.

Overview of Elastically Driven Flow Instabilities

➢ Multidirectional Flows:

Driven Lid Cavity: Localized regions of high normal stresses and streamline curvature.

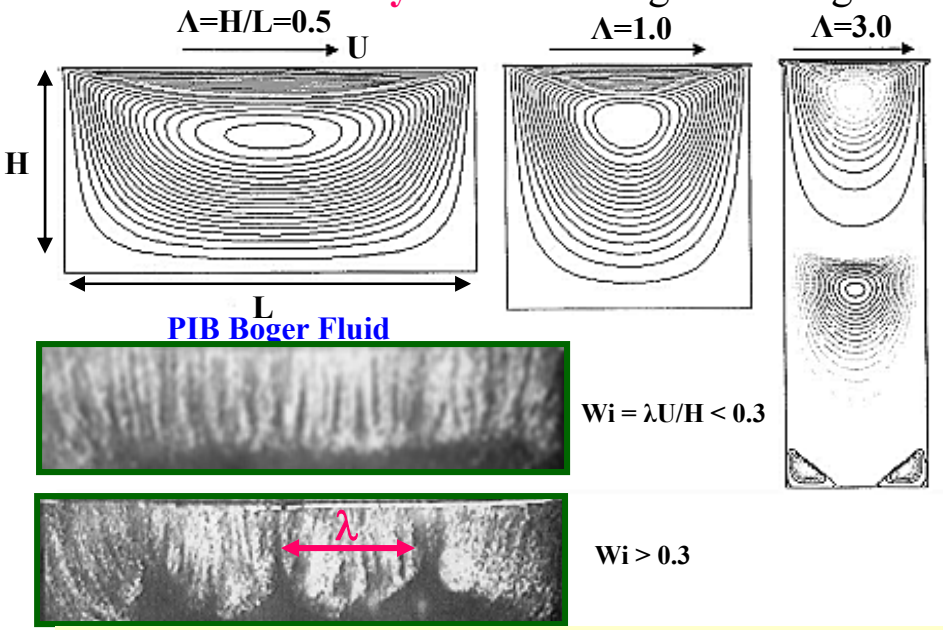

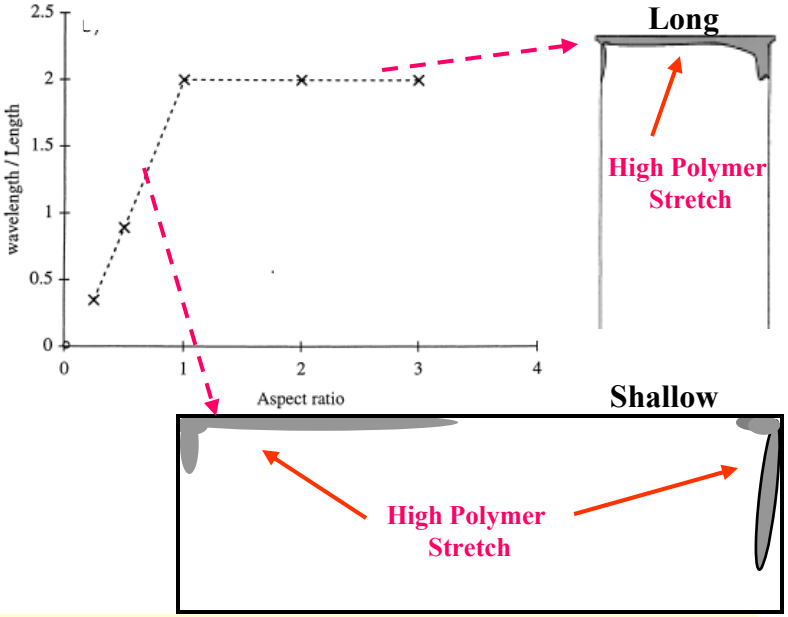

Spatially periodic flow cells that propagate along the neutral direction (Grillet, Yang, Shaqfeh and Khomami (1999, 2000); Pakdel and McKinley 1998).

Viscoelastic Displacement Flows: Localized regions of high normal stress at the interface.

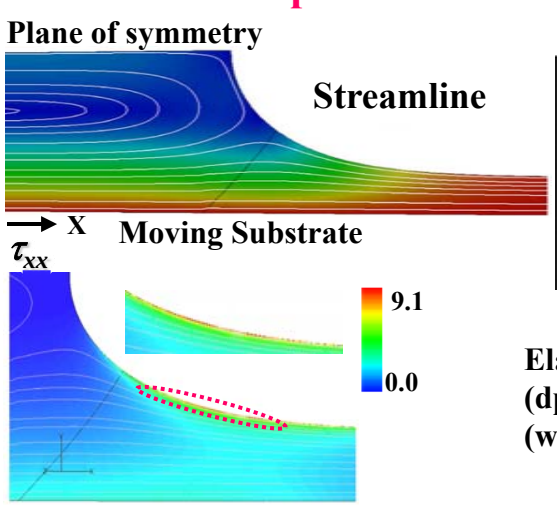

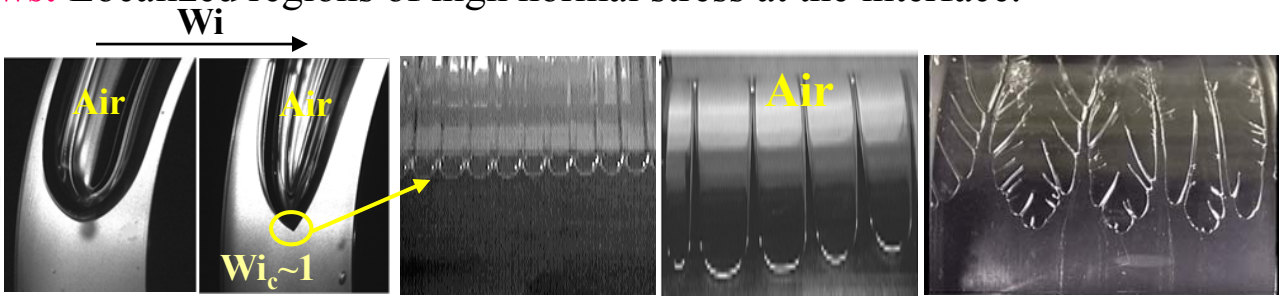

In-plane Transverse

Elastic boundary layer drags significant amount of fluid into films at high Wi, in turn $(dp^+/dx)_{x=x0}$ increases to drive reverse flow. This alters the local conditions to create instability (waves in the transverse direction) at the critical Wi.

Lee, Bhatara, Shaqfeh and Khomami (2000-2005)

Flow Transitions in Viscoelastic Taylor-Couette Flow

There has been significant progress in understanding of onset and mechanism of elastic and thermo-elastic flow instabilities. However, very little is known regarding the post critical dynamics of these instabilities. Transitions in TC flow occurs via a robust sequence of steps. Therefore, investigation of viscoelastic effects on the nonlinear states will not only significantly enhance our understanding of flow-microstructure coupling to shed light on important phenomena such as polymer induced turbulent drag reduction.

Experiments (Groisman, Steinberg (1997,1998))

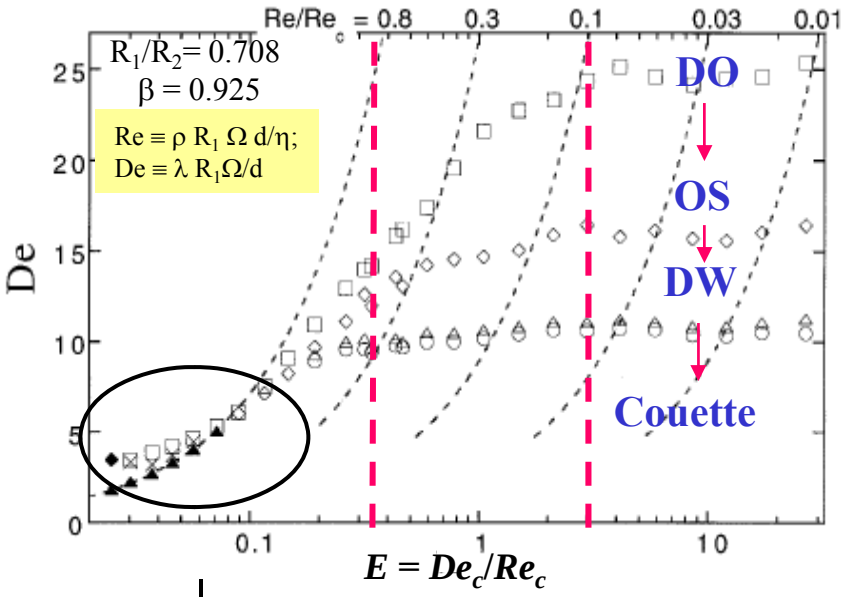

Not very interesting
Couette to TVF

Ribbons (RSW)

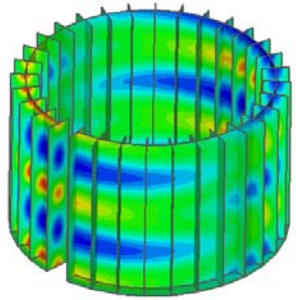

Non-Axisymmetric Oscillatory Strips

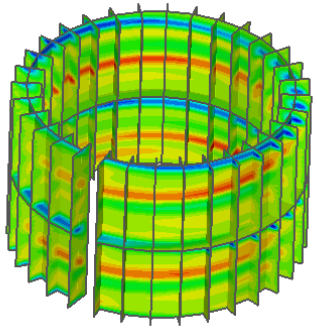

Diwhirls

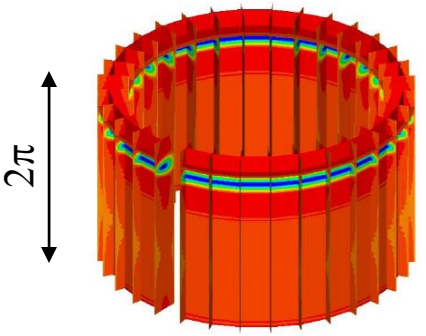

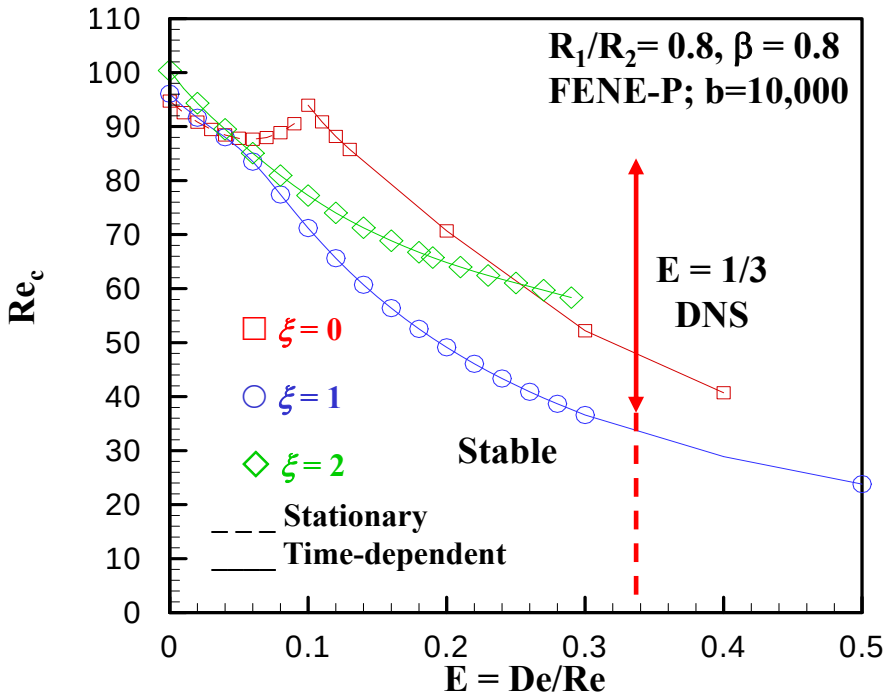

Pattern Formation in Viscoelastic Taylor-Couette Flow: E=1/3

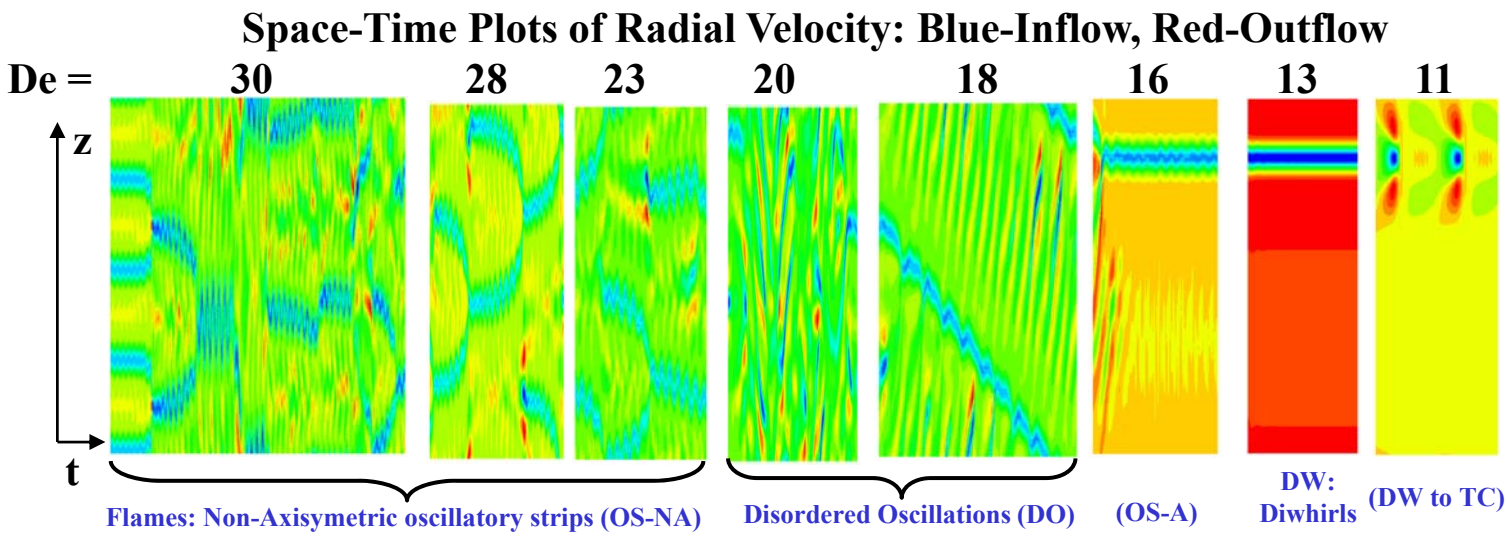

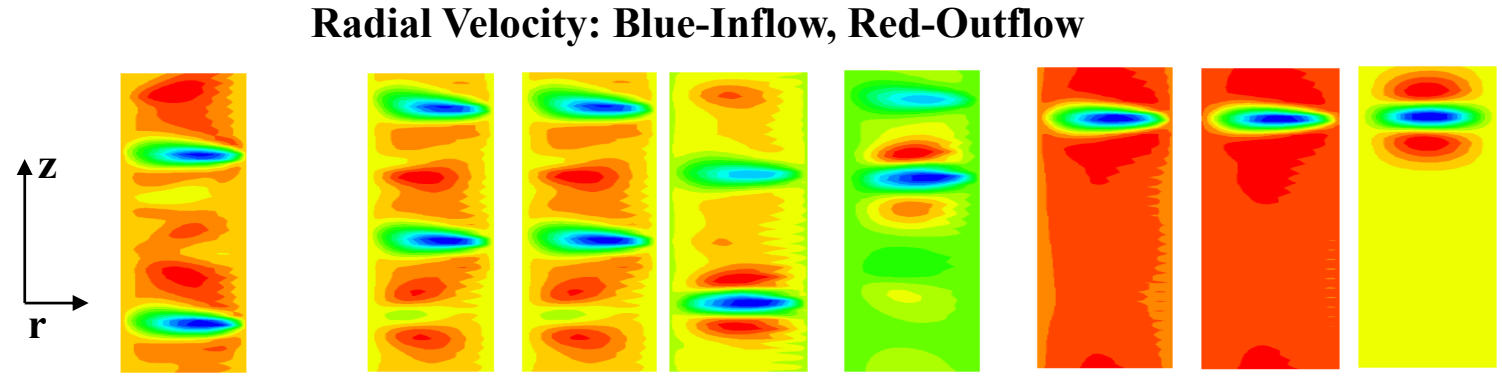

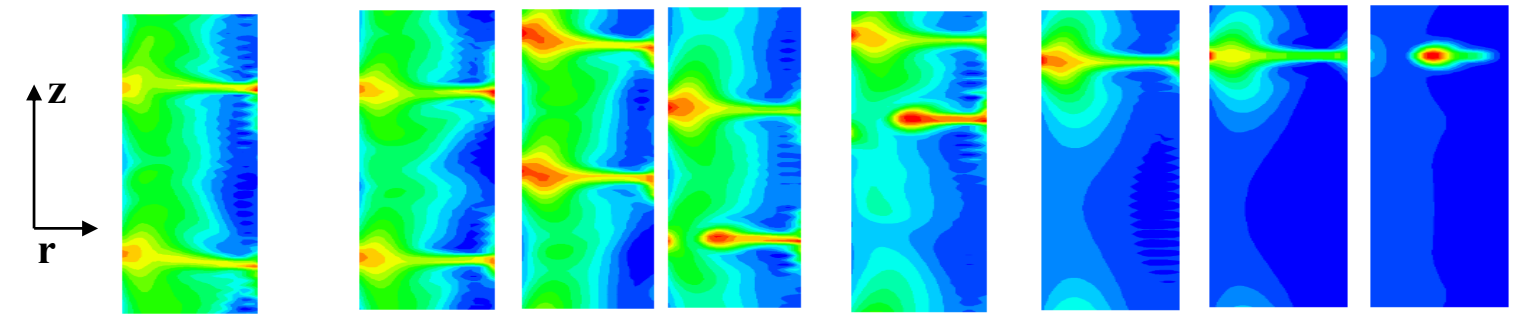

Flow Transitions in Viscoelastic Taylor-Couette Flow: Comparison with Experiments

Experiments (Groisman, Steinberg (1997,1998))

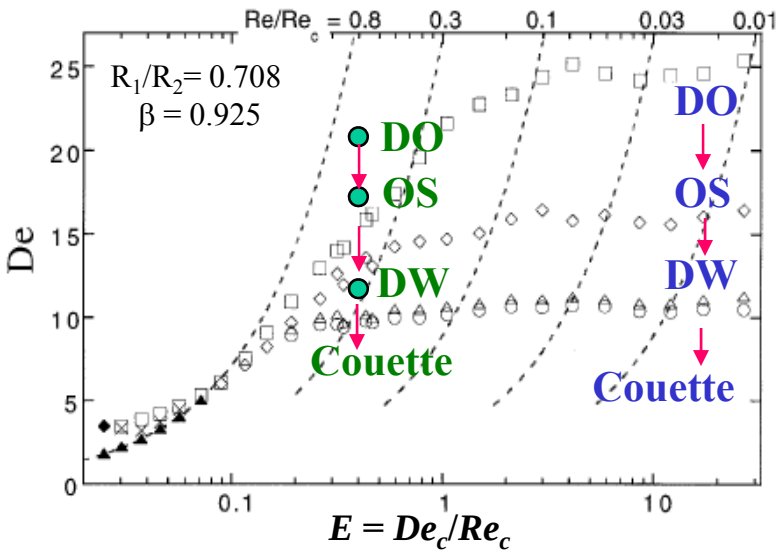

Flames (OS-NA)

Experiments

Baumert and Muller, 1996

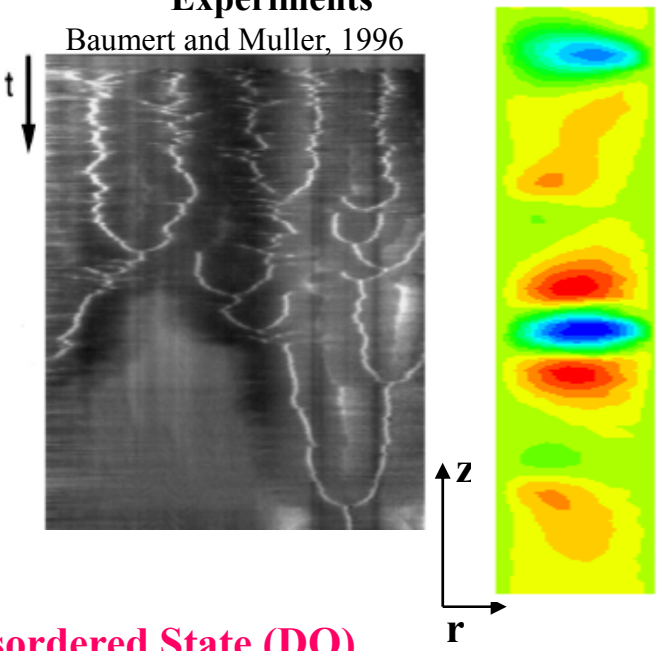

Simulations

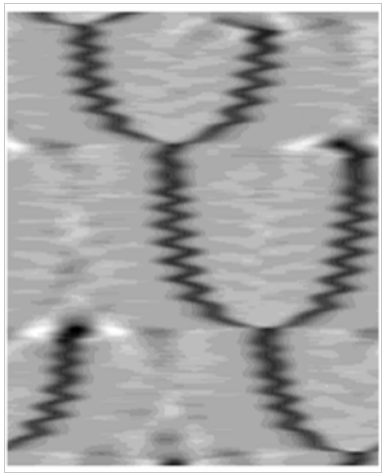

Disordered State (DO)

Space-Time Plots of Radial Velocity

Experiments

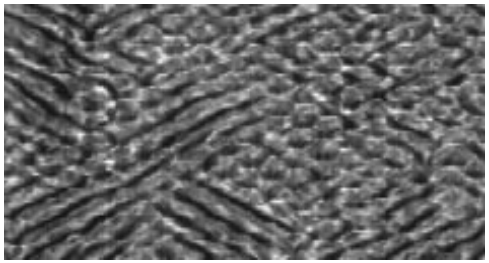

Simulations

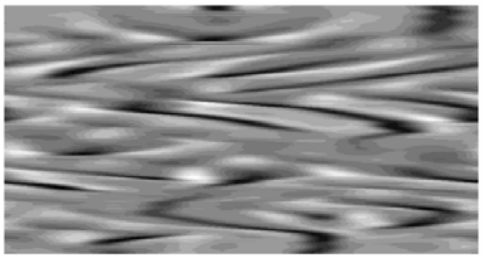

PSD of Radial Velocity

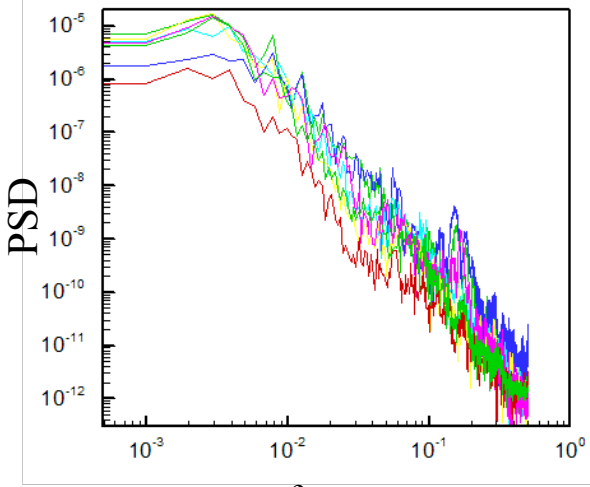

Flow Transitions in Viscoelastic Taylor-Couette Flow: Comparison with Experiments

Diwhirls

Simulations

Experiments
(Groisman and Steinberg,1997)

Radial velocity vs. z
- Strong inflow region
- max to min: 6.5

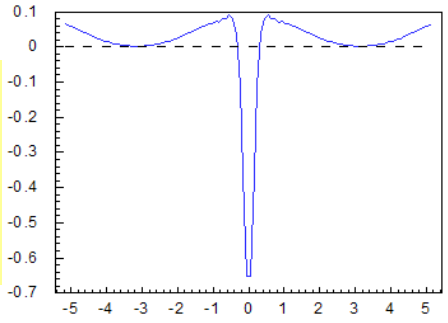

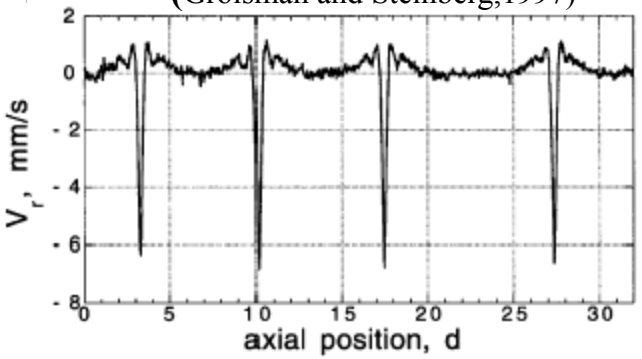

Axial velocity vs. z (near inner wall)
- Inflow splits into upward and downward directions

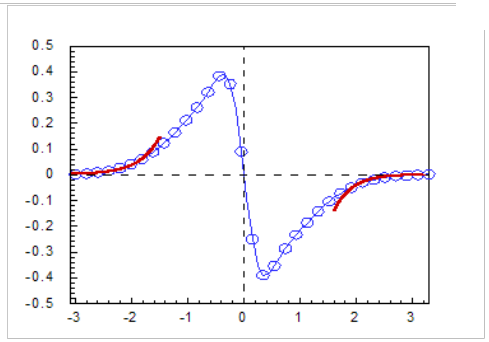

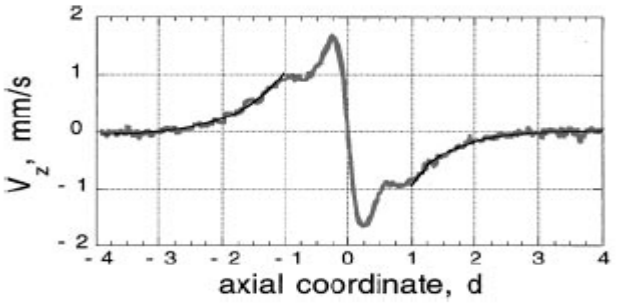

Streamlines

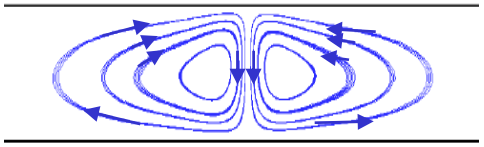

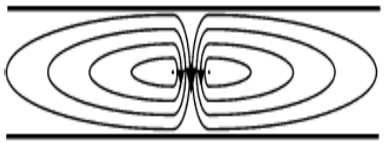

Radial Velocity Contour

Polymer Stretch & Mechanism

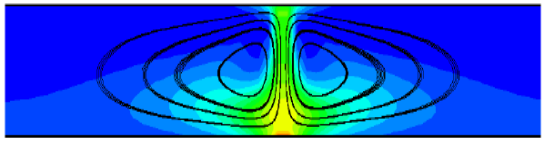

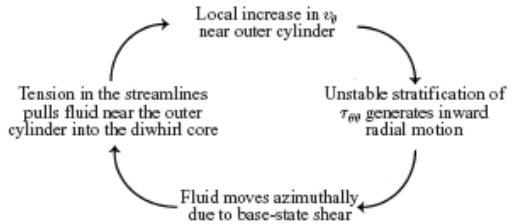

Polymer Induced Turbulent Drag Reduction

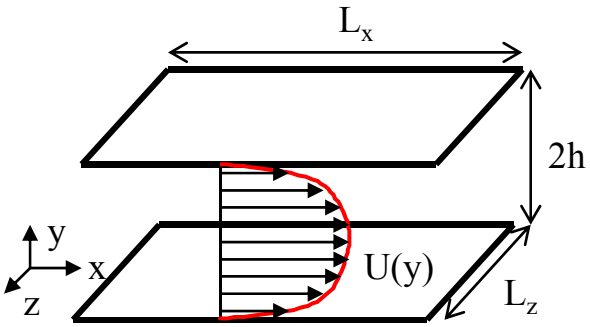

Boundary Conditions:
No-slip and a fixed pressure gradient
FENE-P

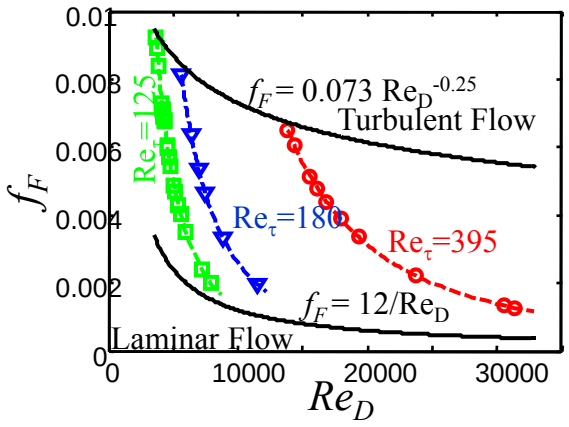

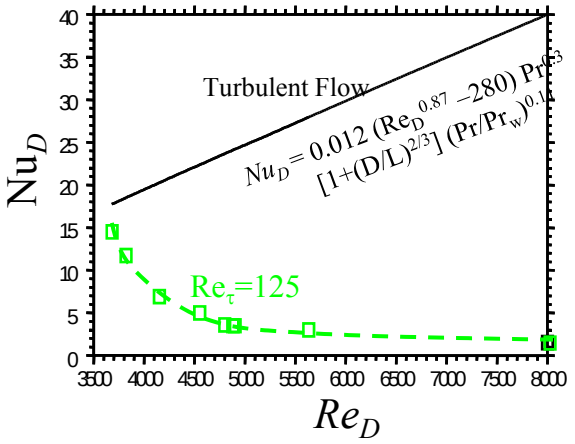

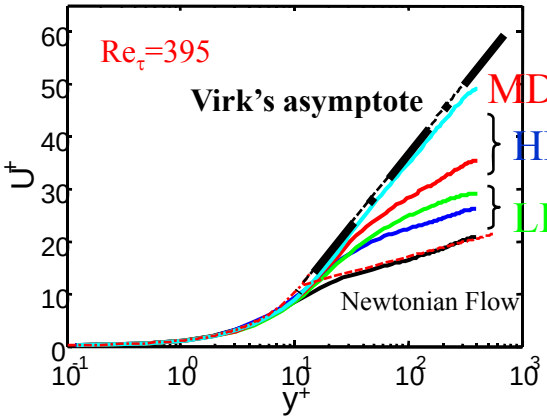

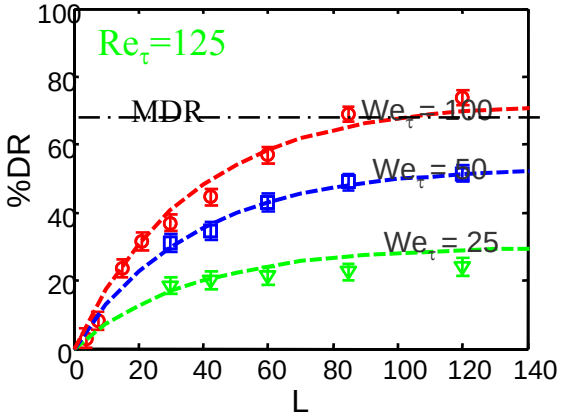

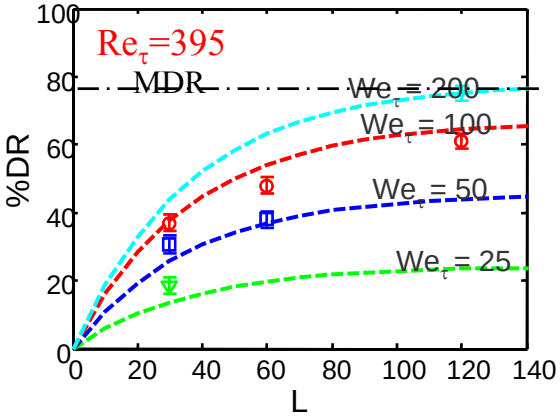

Drag reduction scaling:

$$\%DR = 80 \cdot \left[1 - \exp\left\{-\alpha\left(We_\tau - We_{\tau,c}\right) \cdot \left(\frac{Re_\tau}{Re_{\tau,r}}\right)^{0.225}\right\}\right] \cdot \left[1 - \exp\left(-\beta L\right)\right]$$

Gupta, Surehkumar and Khomami Phys. Fluids (2005);Li, Sureshkumar and Khomami, JNNFM (2006), Li, Gupta, Sureshkumar and Khomami, JNNFM (2006)

Polymer Induced Turbulent Drag Reduction

Re_τ=395, Newtonian Flow

LDR ~ 18%

HDR ~ 50%

MDR ~ 75%

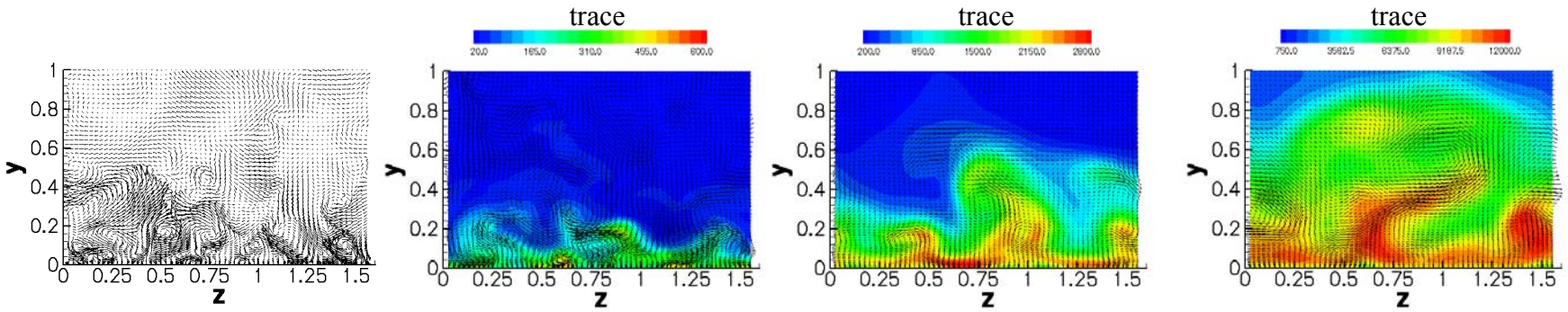

DR

In the near wall region, $\tau_f^+ = 1/\omega_x^+$, rms ~ 5-10

onset of drag reduction $We_\tau \sim 6$

$We_\tau^* \, \omega_x^+$, rms $\sim O(1)$

MDR asymptote

Intricate balance between chain and vortex dynamics results in MDR

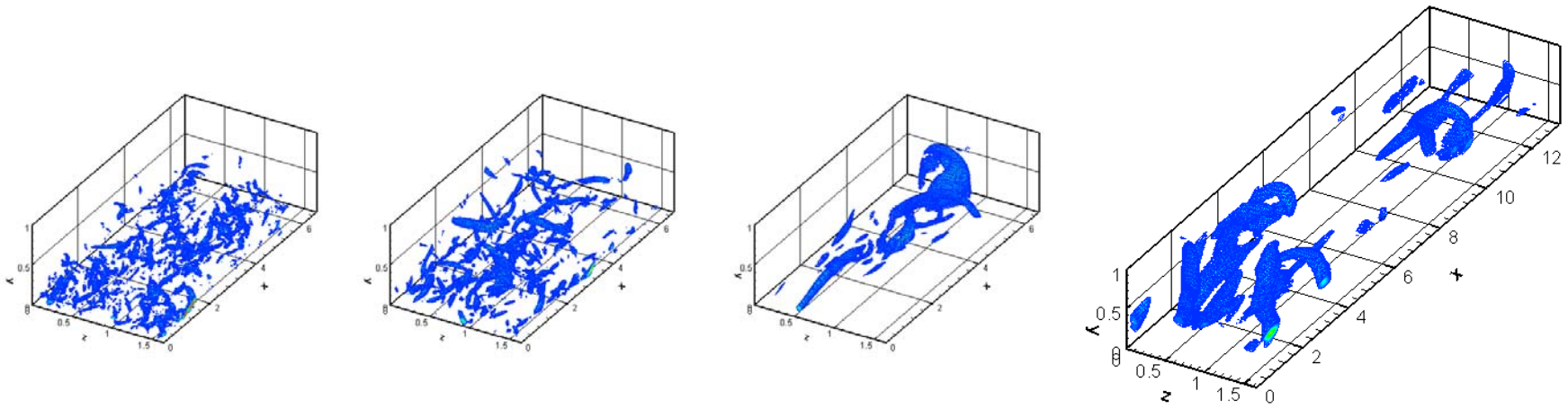

Li, Sureshkumar and Khomami, PRL, submitted (2008)

SUMMARY AND OUTLOOK

Although tremendous progress in large scale flow simulation of polymeric solutions have been made, number of issues deserve further consideration,

- Development of robust and CPU efficient multi-scale simulation strategies based on advanced coarse graining strategies as well as multi-segment description of polymer dynamics.

- Development of hi-fidelity multi-scale simulation techniques for stability analysis of multidimensional flows as well as their post critical dynamics.

- Simulation of complex kinematics confined flows with particular emphasis on micro- and nano-fluidic devices.

ACKNOWLEDGEMENTS

Former and Current Graduate Students and Postdocs

Greg Wilson
Kapil Talwar
Yuan-Yuan Su
Tushar Ganpule
Garth Su
Mohammad Ranjbaran
Bin Yang
Anne Grillet
Alex Lee
Gandharv Bhatara
Usamah Al-Mubaiyedh
Madan Somasi
Anantha Koppol (Multiscale Flow simulations)
Vidya Venkataramani (Configuration model)
Dennis Thomas (Flow transition in viscoelastic TC)
Hoon Sim (Chain Scission)
Vijay Gupta and Chengfeng Li (Turbulent drag reduction)

Colleagues

Radhakrishna Sureshkumar
Eric Shaqfeh

Funding

NSF
ACS-PRF
DARPA
ONR
Mitsubishi
3M
MEMC
SACMI IMOLA